

1959

# Effects of gamma radiation on a transistor RC phase-shift oscillator

Locke, Walter M.

# EFFECTS OF GAMMA RADIATION ON A TRANSISTOR R-C PHASE SHIFT OSCILLATOR

WALTER M. LOCKE
AND
VIRGIL W. MOORE, JR.

# EFFECTS OF GAMMA RADIATION ON A TRANSISTOR R-C PHASE SHIFT OSCILLATOR

* * * * *

Walter M. Locke

and

Virgil W. Moore, Jr.

# EFFECTS OF GAMMA RADIATION ON A TRANSISTOR R-C PHASE SHIFT OSCILLATOR

by

Walter M. Locke
Lieutenant, United States Navy

and

Virgil W. Moore, Jr.
Lieutenant, United States Navy

Submitted in partial fulfillment of
the requirements for the degree of

MASTER OF SCIENCE
IN
ELECTRICAL ENGINEERING

United States Naval Postgraduate School
Monterey, California

1959

# EFFECTS OF GAMMA RADIATION ON A TRANSISTOR R-C PHASE SHIFT OSCILLATOR

by

Walter M. Locke

and

Virgil W. Moore, Jr.

This work is accepted as fulfilling
the thesis requirements for the degree of
MASTER OF SCIENCE
IN
ELECTRICAL ENGINEERING
from the
United States Naval Postgraduate School

ABSTRACT

A transistorized R-C phase shift oscillator was selected for a study of its behavior in a gamma radiation environment. An analysis was made in order to determine the relationships existing between the transistor parameters and the circuit characteristics of the oscillator. Flow graph techniques were used for the circuit network analysis. An application of root locus techniques permitted a graphical interpretation of the characteristic equation obtained for the network. Extension of this work led to the exact formulae and approximations for the starting frequency of both three and four section R-C phase shift oscillators. Predicted values of operating frequency for a given forward current gain of the transistor were compared with experimental results.

Seven identical circuits were irradiated independently in a 1000 curie cobalt-60 gamma flux. The results were displayed as plots of the hybrid parameters of the transistor and the frequency and output voltage of the oscillators as functions of gamma dosage. Normal distribution curves were constructed from the plots of the results. From this information, probability plots were made which expressed the derating of the forward current gain of the transistor and the derating of the frequency and the output voltage of the oscillator as functions of gamma dosage.

The experimental work was performed at the Missiles and Space Division of the Lockheed Aircraft Corporation, Palo Alto, California. The authors desire to express their appreciation for the assistance given by Dr. W. W. Happ and his staff of the Solid-state Electronics Department. We are especially indebted to T. R. Nisbet, N. K. Marshall, and W. E. Price, all of Lockheed, for their suggestions and aid in securing equipment for this work.

In addition, we wish to thank Dr. C. H. Rothauge of the Department of Electrical Engineering, United States Naval Postgraduate School, Monterey, California, for his encouragement and guidance as faculty advisor.

TABLE OF CONTENTS

LIST OF ILLUSTRATIONS

CHAPTER 1

## Background

The advent of the nuclear powered submarine, the travel of missiles and satellites through the radiation belts in space, and the coming of the nuclear powered aircraft have thrown a new environment upon the electronics industry. Radiation effects upon electronic components and systems must be investigated in order to provide systems designers with the limits which may be imposed on them by this environment.

The missile and satellite programs have been "transistorized" in order to accommodate the size and weight limits imposed upon them. Certainly it will be tempting to make extensive use of semiconductors in the nuclear powered aircraft. Consequently, it is important to determine the limiting radiation dose these systems may absorb and still function effectively. It is questionable whether or not it is feasible to use solid-state devices in a strong radiation field, since it is known that semiconductor devices are sensitive to a radiation environment.[1] It would seem, then, that a study of the effects of radiation on solid-state component systems would be of utmost importance.

At this point, it is desirable to define the properties of nuclear radiation and the measuring units used. Alpha particles, beta particles, gamma rays, and neutrons are the primary particles associated with a nuclear reactor.[2] The alpha and beta particles are relatively easily absorbed and do not constitute a radiation damage mechanism. Gamma rays

[1] J. F. Hanson, S. E. Harrison, and W. L. Hood, The Effect of Nuclear Radiation on Electronic Components and Systems, Radiation Effects Information Center, Battelle Memorial Institute, Columbus, Ohio, 1957

[2] J. B. Hoag, et al, Nuclear Reactor Experiments, Van Nostrand, Princeton, N. J., p 12, 14, 66, 1958

and neutrons are much more penetrating and are of prime concern in determining radiation damage.

A. Gamma Rays[2,3,4]

Gamma rays are electromagnetic in nature, like ordinary light. They are of very short wave length and are similar to X-rays, differing in their origin and quantum energy. Gamma rays produce ionization in all solids. There are three distinct processes which account for the energy loss and ionization produced as the gamma rays traverse a material:

1. Photoelectric effect, in which a photon knocks an orbital electron out of an atom and disappears in the process.
2. Compton effect, in which a photon is scattered by a free electron and loses some of its energy in the process.
3. Pair production, in which the photon vanishes and a positron-negatron pair is created.

The total dosage of gamma rays is usually expressed in an ionization measuring unit called the roentgen. The roentgen is defined as the unit gamma dose which produces one electrostatic unit (esu.) of ions of either sign, but not both, in one squared centimeter of dry air measured at standard conditions. It requires 34 electron volts to create one ion pair in standard air; the roentgen is the radiation dose that will release 87.7 ergs of energy in one gram of air.

B. Neutrons

Neutrons are electrically neutral particles of mass. They do not interact with the charged parts of atoms and are therefore very penetrat-

[3]D. Halliday, Introductory Nuclear Physics, 2nd Ed., John Wiley, New York, p 164, 1957

[4]C. T. Dienes and C. H. Vineyard, Radiation Effects in Solids, Interscience Publishers, New York, p 45, 1957

ing. Energy loss is accomplished by collision with atomic nuclei in matter and the resulting slowing down of the particle until it is absorbed in a nuclei, or by decay in free space by beta emission. In free space, the mean life of the particle is 10 minutes; in matter, the particles are usually absorbed before decay can occur.

The measure of the neutron dose rate is referred to as the neutron flux and is expressed as $\phi = nv$. This means the product of the number of neutrons per unit volume n, and their speed v. Unfortunately, the neutrons do not have the same speed and must be defined by the energy ranges:

a. thermal neutron flux (.025 electron volts)

b. resonance neutron flux (1 to 1000 electron volts)

c. fast neutron flux (above .1 mev)

It is common to relate the slow neutron flux and the fast neutron flux as being below or above the speeds or energies at which the absorbtion by cadmium undergoes a very great change in magnitude (about .4 ev). The total neutron dose is measured in terms of integrated flux, nvt, which is expressed as the number of neutrons per square centimeter.

## CHAPTER 2

## Radiation Effects Upon Components

The study of radiation effects upon semiconductor materials and devices has been the work of many experimentors. The general research pattern followed has been first to define the changes in the semiconductor materials, germanium and silicon, caused by radiation; and secondly, to study radiation effects on various transistors and diodes.

According to Pigg and Robinson[5], the damage mechanism to semiconductor material exposed to the radiation field in a nuclear reactor may be classified according to neutron and gamma ray effects.

A. Neutron Damage

1. Transmutation is produced by the capture of thermal neutrons. The subsequent radioactive decay introduces a chemical impurity into the crystal lattice.

2. The inelastic scattering of high energy neutrons produces a lattice disorder.

B. Gamma Ray Damage

1. Compton scattering of gamma photons results in high-energy electrons which can produce lattice disorder by elastic scattering.

2. Photoelectric and photoconductivity effects are present and may affect the operation of a given circuit.

It is noted that annealing which may or may not tend to return the semiconductor material toward its initial condition occurs for all temperatures above 130 degrees K.

[5]J. C. Pigg and C. C. Robinson,"Radiation Effects in Semiconductor Devices," from Proceedings of the Transistor Reliability Symposium, September 17 and 18, 1956, New York University Press, 1958

Radiation damage to the semiconductor materials germanium and silicon may be summarized:

a. Irradiation of germanium converts n-type material into p-type material.

b. Irradiation of silicon reduces the conductivity of p-type and n-type material monatonically.

The damage to transistors and diodes by radiation may now be described. These semiconductor devices are made up of one or more barriers between p-type and n-type material. Germanium devices simply become a lump of p-type germanium after absorbing a sufficient radiation dose. Silicon devices are destroyed as the conductivity of the materials decreases.

The findings of Steele may be summarized for gamma ray effects on transistors:[6]

a. Irradiation by cobalt-60 gamma rays at fluxes in excess of $10^3$ roentgen/hour and at doses greater than $10^6$ roentgen is necessary to induce temporary and permanent effects in transistor parameters.

b. As the transistor radiation damage increases, there are two general effects noted. There is a fall in current gain, $h_{fe}$, and a rise in the leakage current, $I_{co}$.

Radiation effects on other electronic components have been compiled by the Battelle Memorial Institute.[7] Some important ones are:

a. Resistors. Wire wound resistors are by far the most

[6]H. L. Steele, Jr.,"Effects of Gamma Radiation on Transistor Parameters," Proceedings of the Transistor Reliability Symposium, September 17 and 18, 1956, New York University Press, New York, 1958

[7]J. F. Hanson, S. E. Harrison, and W. L. Hood, The Effect of Nuclear Radiation on Electronic Components and Systems, The Radiation Effects Information Center, Battelle Memorial Institute, Columbus, Ohio, 1957

radiation resistant.

b. Capacitors. Mica, glass, and ceramic capacitors suffer little damage while plastic, electrolytic, and oil filled types are extremely susceptable to damage.

c. Tubes. Tubes are usable in a radiation field. The largest cause of tube failure is envelope and seal fracture caused by the use of borosilicate glasses.

CHAPTER 3

## Circuit Selection

It has been pointed out that considerable work has been accomplished in the study of radiation effects on solid-state components. The study of the radiation effects on any large electronic system is not practical from the stand point that most nuclear reactors and gamma facilities have but small areas available in which the flux pattern is uniform. A study of the radiation effects on any given system must be based on the knowledge of damage to basic circuits comprising the system such as amplifiers, oscillators, multivibrators, and pulse shaping circuits. Such circuits can be made small enough to fit in the limited uniform flux areas available.

The testing of semiconductor devices in a gamma ray radiation environment has been done by the Boeing Airplane Company. One report[8] states a finding that a semiconductor sine wave oscillator exhibited extremely stable operation for exposure times of several minutes, while a blocking oscillator operated for only a few seconds when exposed to the same flux. On the basis of this work and the results reported by the other experimentors in the previous chapter, it becomes apparent that considerable differences exist in the radiation damage to semiconductor devices. In particular, damage to a specific type of device made by the same manufacturer will vary widely for the number tested.

It may be reasoned, then, that for any given circuit using solid-state components, the radiation effects on identical circuits may be expected to show marked differences. Also, it can be stated that the success or failure

[8]G. L. Keister and H. V. Stewart,"Preliminary Report of an Investigation of the Effects of Nuclear Radiation on Selected Transistors and Diodes," Boeing Airplane Company Report D5-1183, dtd 22 August 1956

of any circuit using semiconductor components when exposed to a radiation environment is a function of the dependence of that particular circuit on the semiconductor components.

The authors selected the transistor R-C phase shift oscillator as shown in Fig. 3-1 for a study of its operation in a radiation environment for the following reasons:

a. At the present time, the most widely used frequency division telemetering system is the FM-FM system which utilizes R-C phase shift, L-C, and multivibrator type subcarrier oscillators.[9]

b. The circuit shown in Fig. 3-1 is being used in industry for various missile applications.[10]

c. Temperature effects upon this particular circuit have been noted. The oscillator continued operation over a very wide temperature range with an ensuing large beta change. It was anticipated that such a circuit would have a long life in a radiation field where beta decay in a transistor is one of the known damages to a transistor.

d. The circuit lends itself to linear circuit theory.

e. The circuit uses the Texas Instrument 904 transistor which has been irradiated in a 1500 curie cobalt-60 gamma field by another investigator.[8]

The R and C components selected for use in the circuit were wire wound resistors and mica capacitors. Both types of material have been found to be relatively radiation resistant. The 18 uf capacitor was not critical

[9]M. H. Nichols and L. L. Rouch, Radio Telemetry, 2nd Ed., John Wiley, New York, p 253, 1956

[10]Circuit provided by Mr. N. K. Marshall, Research Scientist, Lockheed Missile Systems Division, Palo Alto, California

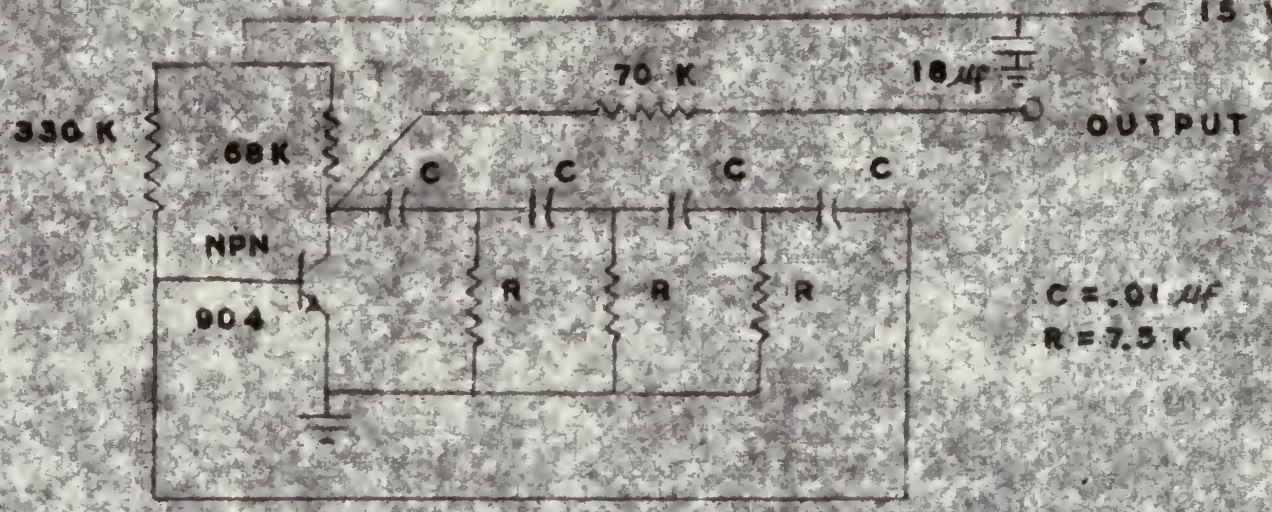


FIG. 3-1 R.- C. PHASE SHIFT OSC.

to the operation of the circuit and because of its size it was mounted outside the radiation chamber on the control panel.

Some comment should be made at this time concerning the types of radiation facilities available. A nuclear reactor has a radiation field consisting of integrated slow and fast neutrons and gamma rays. The calibration of the radiation field is difficult because the flux is not constant. Radioactive particle contamination is a problem and hampers any instrumentation of circuits or material introduced into the radiation field.

Certainly, systems which are to be operated within the environment of a nuclear reactor should be investigated within that environment, but a more exhaustive approach to the analysis of the same system would be provided by a study of the damage to that system by the individual types of radiation particles separately.

A gamma facility was selected for this investigation not only for the above reasoning but also for its non-contamination feature and ease of instrumentation.

CHAPTER 4

ANALYSIS

THE FUNCTION OF THE TRANSISTOR IN A PHASE SHIFT OSCILLATOR

A. SCOPE

In the course of the investigation of the radiation effects on a transistor phase-shift oscillator the authors found a need for knowledge of the function of the transistor in the oscillator operation. It is known that the transistor is more sensitive to gamma radiation than resistors or capacitors.[1] Further, the components other than the transistor can be easily selected so that they will be essentially unaffected by radiation up to the level of junction transistor destruction. Data are available on the effects of gamma radiation on many transistors making possible the prediction of parameter variation.[8] But how will the frequency of the phase-shift oscillator vary? To answer this, one must know the relationship of the transistor parameters to the rest of the circuit.

A search of the literature revealed that the vacuum tube version has been well analyzed.[11-15] Despite this pioneering work, the several analyses of the transistor phase-shift oscillator were found to be not

[11] E. L. Ginzton and L. M. Hollingsworth, "Phase-Shift Oscillators," Pros. I.R.E., 29, 43-49, February 1941

[12] M. Artzt, "Frequency Modulation of Resistance-Capacitance Oscillators," Proc. I.R.E., 32, 409-414, July 1944.

[13] W. C. Vaughn, "Phase-Shift Oscillator", Wireless Eng., 26, 391-399, December 1949.

[14] W. R. Hinton, "The Design of R. C. Oscillator Phase Shifting Networks", Electronic Eng., 22, 13-17, January 1950.

[15] S. Sherr, "Generalized Equations for R C Phase-Shift Oscillators," Proc. I.R.E., 42, 1169-1172, July 1954.

as general or as complete as the studies of the vacuum tube phase-shift oscillator; and, as a consequence, did not satisfy the problem.[16-20] It was therefore necessary to make a complete analysis with the goal of finding the change in frequency of a phase-shift oscillator with variation in the transistor parameters. While this goal was admittedly limited, the methods to be described can be used to study the variation in frequency with changes of passive network values.

B. CIRCUIT CONFIGURATION

Any phase-shift oscillator can be represented by the over simplified block diagram of Fig. 4-1. The passive network is usually a three or four section ladder with capacitors as the series elements, and resistors as the shunt elements, or vice versa. Each RC combination is called a section or a step. Sometimes the transistor impedances are considered as forming part of a section. Capacitors are usually chosen instead of inductors because of their small physical size and losslessness for the low audio frequency range.

In considering what circuit configuration to use, it was found that for tubes the passive network for a RC phase-shift oscillator had been generalized to the network shown in Fig. 4-2.[15] This is for an

[16] W. Hicks, "Transistor Phase-Shift Oscillator," Tele-Tech and Electronic Industries, 55-56, July 1956

[17] R. P. Turner, "Transistorized Phase-Shift Oscillator," Radio and Television News, p. 108, April 1956

[18] R. F. Shea, et al, Transistor Circuit Engineering, McGraw-Hill, New York, 1957

[19] E. Wolfendale, The Junction Transistor and its Applications, Heywood and Company LTD., London 1958

[20] V. M. Luibin, "Transistor RC-Oscillators with Phase Reversal," Radio Engineering, 13, 2, 60-69, Translated by Porgonan Institute, New York, 1958

as general or as complete as the studies of the vacuum tube phase-shift oscillator; and, as a consequence, did not satisfy the problem.[16-20] It was therefore necessary to make a complete analysis with the goal of finding the change in frequency of a phase-shift oscillator with variation in the transistor parameters. While this goal was admittedly limited, the methods to be described can be used to study the variation in frequency with changes of passive network values.

B. CIRCUIT CONFIGURATION

Any phase-shift oscillator can be represented by the over simplified block diagram of Fig. 4-1. The passive network is usually a three or four section ladder with capacitors as the series elements, and resistors as the shunt elements, or vice versa. Each RC combination is called a section or a step. Sometimes the transistor impedances are considered as forming part of a section. Capacitors are usually chosen instead of inductors because of their small physical size and losslessness for the low audio frequency range.

In considering what circuit configuration to use, it was found that for tubes the passive network for a RC phase-shift oscillator had been generalized to the network shown in Fig. 4-2.[15] This is for an

[16] W. Hicks, "Transistor Phase-Shift Oscillator," Tele-Tech and Electronic Industries, 55-56, July 1956

[17] R. P. Turner, "Transistorized Phase-Shift Oscillator," Radio and Television News, p. 108, April 1956

[18] R. F. Shea, et al, Transistor Circuit Engineering, McGraw-Hill, New York, 1957

[19] E. Wolfendale, The Junction Transistor and its Applications, Heywood and Company LTD., London 1958

[20] V. M. Luibin, "Transistor RC-Oscillators with Phase Reversal," Radio Engineering, 13, 2, 60-69, Translated by Porgonan Institute, New York, 1958

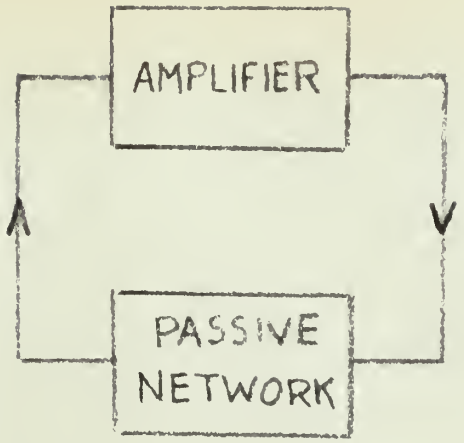


Block Diagram of a Phase-Shift Oscillator

Fig. 4-1

---

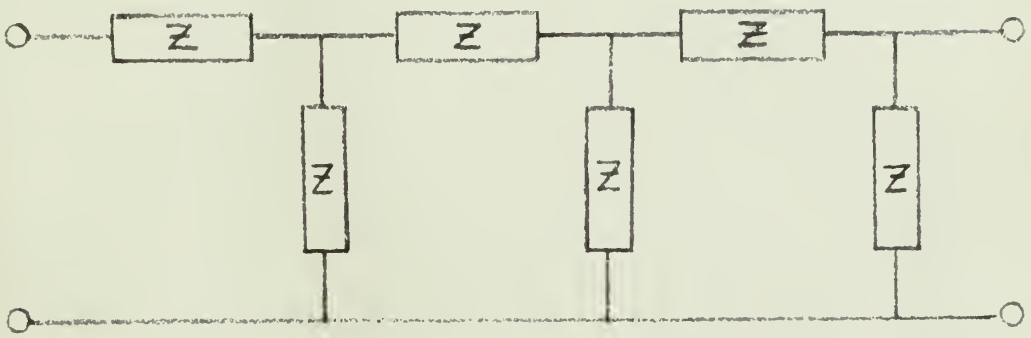


Generalized Phase-shifting Network for Voltage Amplifiers

Fig. 4-2

---

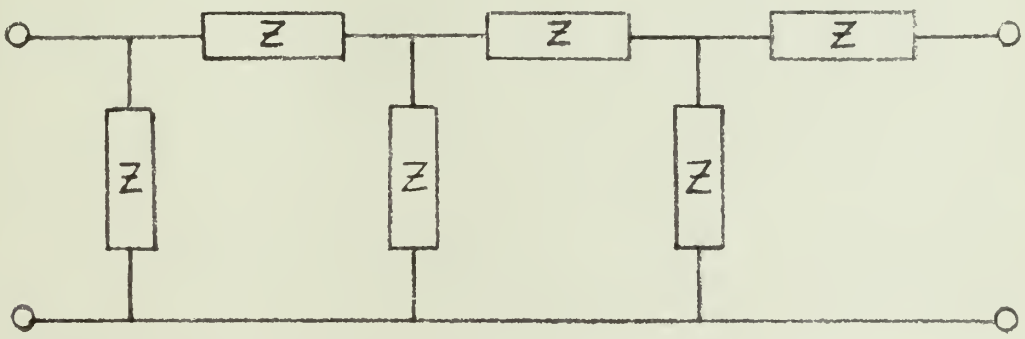


Generalized Phase-shifting Network for Current Amplifiers

Fig. 4-3

ideal voltage amplifier with low output and high input impedance. The transistor in the grounded emitter configuration approaches an ideal current amplifier with high output and low input impedance; therefore, the passive network should be of the form shown in Fig. 4-3.[19]

While this duality seems obvious, many designers have inadvertently used the wrong network in their efforts to bias the transistor with the result of no oscillations or of high gain requirements to produce oscillations.

The circuit analyzed had four sections and is shown in Fig. 4-4. For convenience of design, the shunt elements were chosen as resistors so that the normal load resistor of an amplifier stage formed part of the passive network.

C. LINEAR ANALYSIS OF OSCILLATOR

This circuit can best be studied by constructing a mathematical model from equivalent circuit as drawn in Fig. 4-5. However, first consider some of the things known about the phase-shift oscillator. It has a more or less sinusoidal output; for this analysis it will be considered to have a perfect sinusoidal output. This consideration anticipates the assumption that the circuit is linear. The nonlinear action of the transistor will only be considered as a limit on the transistor characteristics. The circuit as represented by linear incremental model is shown in Fig. 4-6.

Of any linear sinusoidal oscillator the following observations can be made:[21,22]

[21]W. Edson, Vacuum Tube Oscillators, John Wiley, New York, 1953

[22]R. B. Hurley, Junction Transistor Electronics, John Wiley, New York, 1958

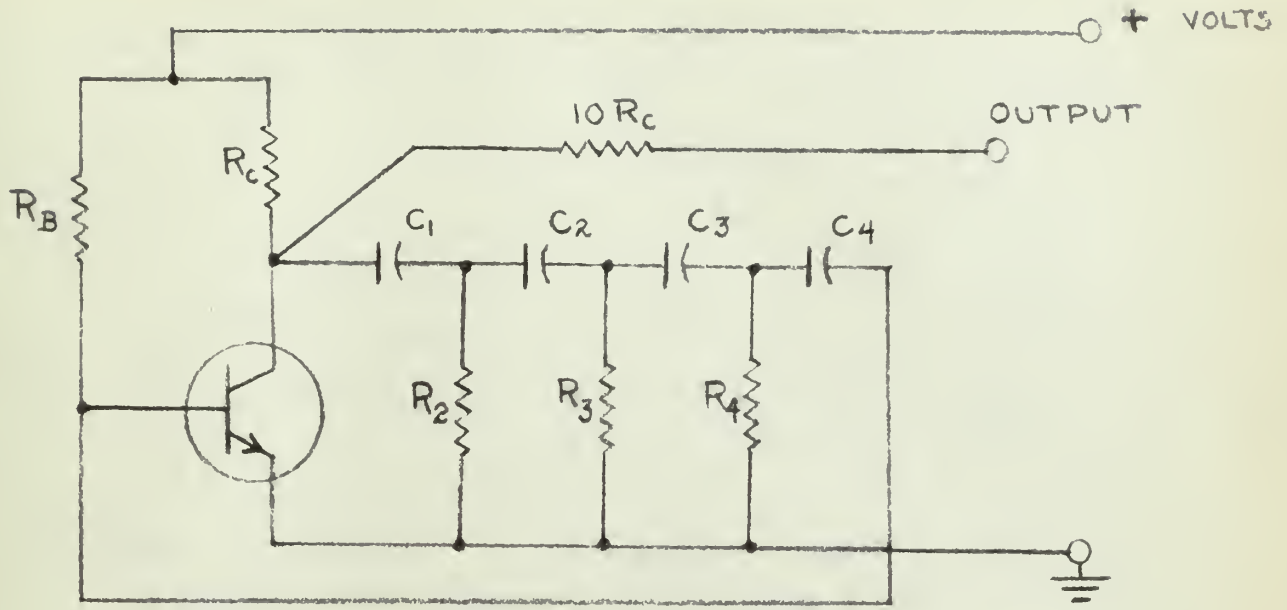


Four Section Transistor Phase-shift Oscillator
Fig. 4-4

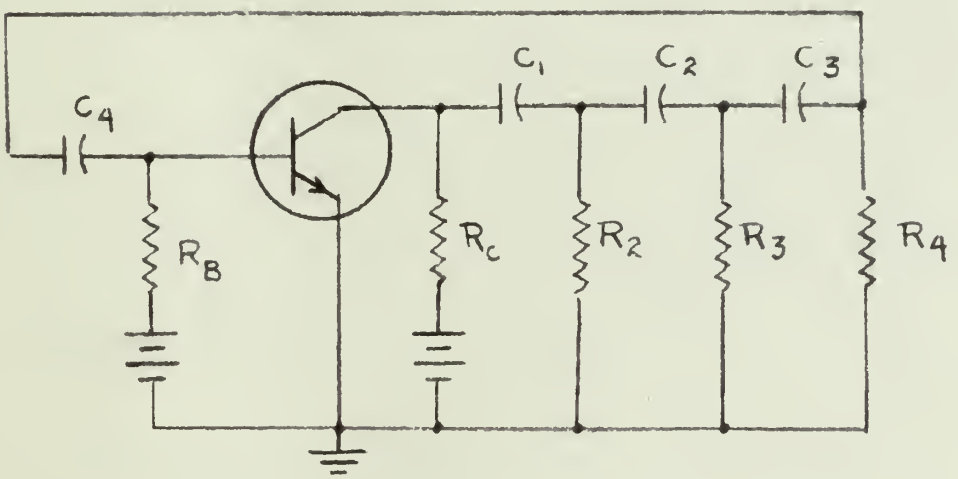


Equivalent Circuit
Fig 4-5

1. that natural oscillations can be set up in a circuit by the introduction of a random impulse, $u_i$ (t);
2. that the natural oscillations are observed in all locations of the circuit simultaneously;
3. that the random pulse to start oscillation can originate or imagine to be introduced at any point in the circuit;
4. that the natural oscillations of a linear system are independent of initial energy storages in the reactive elements;
5. that the natural oscillations of a linear system are determined by the denominator of the transfer function of the system. This denominator is also referred to as the characteristic polynomial of the system.

The characteristic polynomial of the linear incremental model of the transistor phase-shift oscillator can be found by systematic circuit analysis; i.e., mesh, nodal, or matrix methods. However, in this paper, flow graph analysis as summarized in Appendix I will be used.[23-28] With flow graph analysis, quantities can be rearranged without loss of their interrelationships; assumptions can be readily justified; the effect of neglecting any parameter can be easily observed; and finally, the form of the topology equation is convenient for root locus plotting.[23,29]

[23] S. J. Mason, "Feedback Theory--Some properties of Signal Flow Graphs", Proc. I.R.E., 41, 9, p. 1144, 1953

[24] J. G. Truxal, Automatic Feedback Control System Synthesis, McGraw-Hill, 1955

[25] S. J. Mason, "Feedback Theory--Further Properties of Signal Flow Graphs", Proc. I.R.E., 44, 7, p. 920, 1956

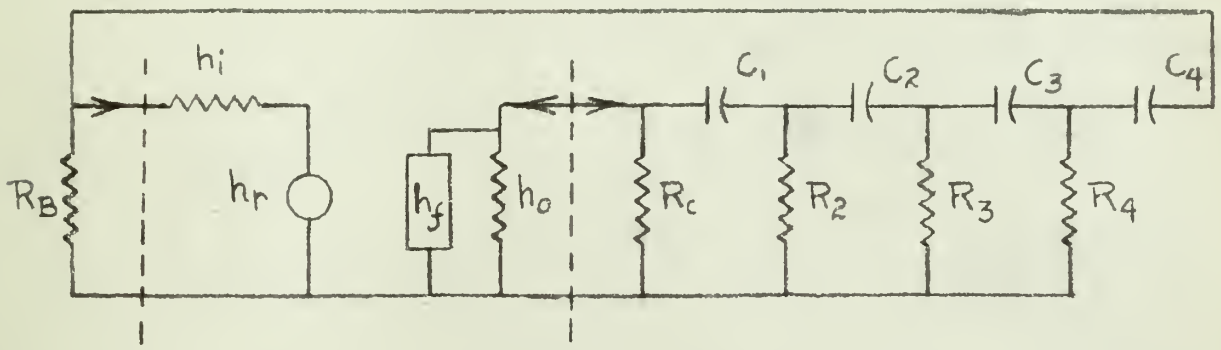


Incremental Linear Model

Fig. 4-6

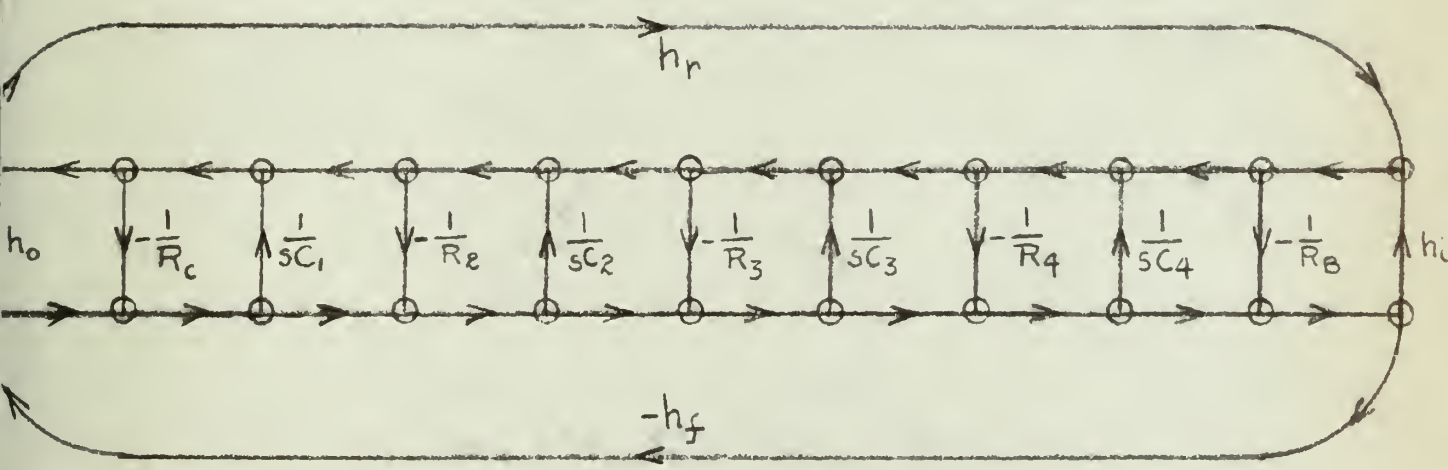


Flow-graph of Transistor, RC Phase-shift Oscillator

Fig. 4-7

D. DETERMINING THE EQUATION CHARACTERISTIC OF THE CIRCUIT

The flow graph of Fig. 4-7 was constructed by a method described in Appendix I. As it was anticipated that the change in current gain, $h_{fe}$, would cause the greatest effect on the oscillator characteristics, the flow graph was arranged so that the transistor current gain formed an exterior loop.

Some simplifications were made because this analysis was interested in the variation of transistor parameters and not those of the other components.

Let $$C_1 = C_2 = C_3 = C_4 = C \qquad (1)$$

$$\frac{1}{R_1} = \frac{1}{R_2} = \frac{1}{R_3} = \frac{1}{R_4} = \frac{1}{R} \qquad (2)$$

where $$\frac{1}{R_1} = \left(h_o + \frac{1}{R_c}\right) \text{ by design} \qquad (3)$$

These simplifications were incorporated in Fig. 4-8.

The equation characteristic of any closed flow graph is the topology equation.

$$\sum_{n=0}^{\infty} (-1)^n L_n = 0 \qquad (4)$$

where $L_n \triangleq$ Loops of $n^{th}$ order that exist in a given flow graph

and $L_o \triangleq 1$.

[26] O. Ming, "Ladder Network Analysis by Signal Flow Graphs", Trans. I.R.E., P.G.C.T., CT-3, p. 289, 1956

[27] W.W. Happ, "Signal Flow Graphs", Proc. I.R.E., 45, 9, p. 1293, 1957

[28] T.R. Nesbit and W.W. Happ, "Flow Graph Analysis", Lockheed Missiles and Space Division, LMSD-48357, Sunnyvale, California, 31 December 1958

[29] W.R. Evans, Control System Dynamics, McGraw-Hill Book Co., Inc. New York, 1954

The topology equation yielded for the flow graph of Fig. 4-8:

$$\left(1+\frac{h_{ie}}{R_B}\right)\left[1+\frac{10}{sCR}+\frac{5}{(sCR)^2}+\frac{7}{(sCR)^3}+\frac{1}{(sCR)^4}\right]$$

$$+\left(\frac{h_{ie}}{R}\right)\left[4+\frac{10}{sCR}+\frac{6}{(sCR)^2}+\frac{1}{(sCR)^3}\right]+h_{fe}(1-h_{re})-h_{re}=0 \qquad (5)$$

Typical circuit parameter values are listed in Table I. The transistor used was a Texas Instrument 904.

Table I

| $h_{ie}$ | $h_{re}$ | $h_{fe}$ | $h_{oe}$ | $R_c$ | $R_B$ | C | R | $h_{ie}/R$ | $h_{ie}/R_B$ |
|---|---|---|---|---|---|---|---|---|---|
| 2K Ω | $8\times10^{-4}$ | 35 | 20 mho | 6.8KΩ | 330KΩ | .01 uf | 6K Ω | $\frac{1}{3}$ | $1.8\times10^{-2}$ |

obviously $\frac{h_{ie}}{R_B} \ll 1$ (6)

and $h_{re} \lll 1$ (7)

This approximated the equation to:

$$\left[1+\frac{10}{sCR}+\frac{15}{(sCR)^2}+\frac{7}{(sCR)^3}+\frac{1}{(sCR)^4}\right]+\left(\frac{h_{ie}}{R}\right)\left[4+\frac{10}{sCR}+\frac{6}{(sCR)^2}+\frac{1}{(sCR)^3}\right]$$

$$+h_{fe}=0 \qquad (8)$$

which is characteristic of the approximate flow graph shown in Fig. 4-9. The dotted partitions were put in to emphasize the correspondence with Fig. 4-1.

E. DERIVATION OF THE GENERALIZED EQUATION FOR N SECTIONS

For the four section, transistor, RC phase-shift oscillator, the following form was derived by application of the topology equation:

$$f_1(sCR)+\left(\frac{h_{ie}}{R}\right)f_2(sCR)+h_{fe}=0 \qquad (9)$$

where $f_1$ and $f_2$ are as shown in Table II.

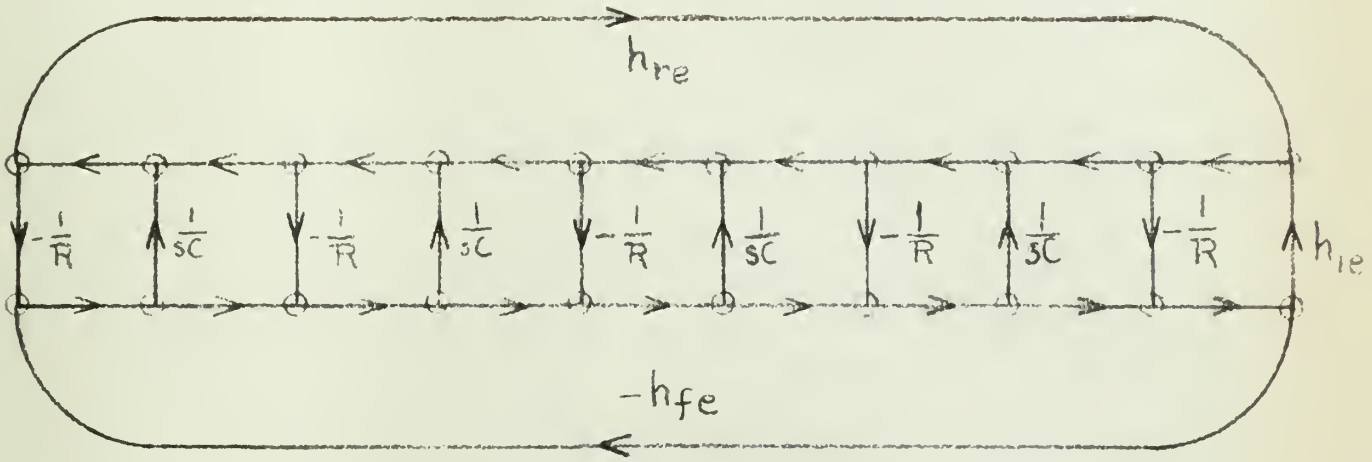


Simplified Flow-graph

Fig. 4-8

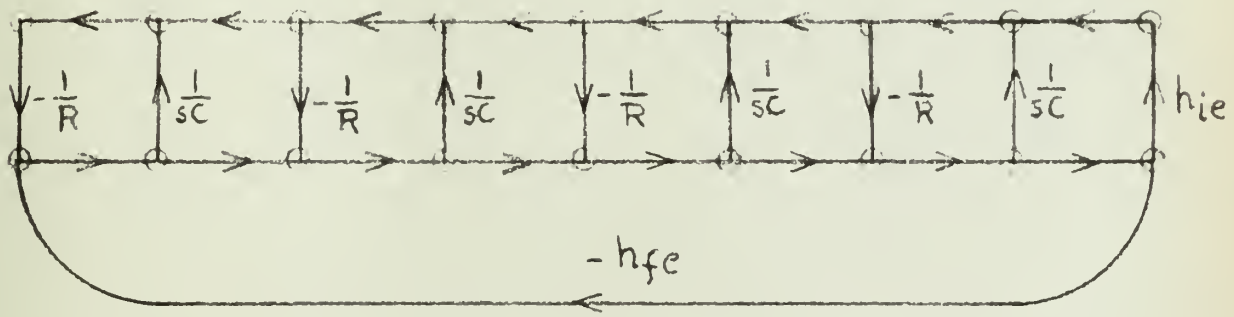


Approximate Flow-graph

Fig. 4-9

Table II

Functions obtained for n sections

| Sections | $f_1$ | $f_2$ |
|---|---|---|
| 1 | $1 + \frac{1}{sCR}$ | 1 |
| 2 | $1 + \frac{3}{sCR} + \frac{1}{(sCR)^2}$ | $2 + \frac{1}{sCR}$ |
| 3 | $1 + \frac{6}{sCR} + \frac{5}{(sCR)^2} + \frac{1}{(sCR)^3}$ | $3 + \frac{4}{sCR} + \frac{1}{(sCR)^2}$ |
| 4 | $1 + \frac{10}{sCR} + \frac{15}{(sCR)^2} + \frac{7}{(sCR)^3} + \frac{1}{(sCR)^4}$ | $4 + \frac{10}{sCR} + \frac{6}{(sCR)^2} + \frac{1}{(sCR)^3}$ |
| n | $\sum_{j=0}^{n} \binom{n+j}{n-j} \left(\frac{1}{sCR}\right)^j$ | $\sum_{j=0}^{n} \binom{n+j}{n-j-1} \left(\frac{1}{sCR}\right)^j$ |

The above table may also be extended by observing that

$$f_{1(n-1)} + f_{2(n-1)} = f_{2n}$$

and

$$f_{1(n-1)} + \left(\frac{1}{sCR}\right) f_{2n} = f_{1n}$$

Noting the binomial cofficients, a generating function was derived to produce the topology equation for n section flow graphs of the configuration of Fig. 4-9.

$$\sum_{p=0}^{1} \sum_{j=0}^{n} \binom{n+j}{n-j-p} \left(\frac{1}{sCR}\right)^{j} \left(\frac{h_{ie}}{R}\right)^{p} + h_{fe} = 0 \qquad (10)$$

where $\binom{a}{b} \triangleq \frac{a!}{b!(a-b)!}$ ; $0! \triangleq 1$ ; $\frac{m!}{-1} \triangleq 0$

n = number of sections or steps in ladder network.

From this generating function, $f_1$ and $f_2$ for n sections are listed in Table II. To verify, $f_1$ and $f_2$ for three sections were listed and compared with the result by flow graph analysis. The function for n = 1, 2 and 5 are also listed; but it should be recalled from experience that only when n = 3 or 4 is a phase-shift oscillator possible. For n = 1 only a damped exponential is possible. If n = 2 it is possible to produce damped oscillations with sustained oscillations theoretically produced with infinite current gain, $h_{fe}$. With n = 5 or more, multiple oscillations are possible summing to a distorted wave. If these statements are not intuitively reasonable, they will become so with study of the root loci of the topology equations.

## 4. ROOT LOCUS OF THE CIRCUIT

The location of the roots of the topology equation in the s plane are indicative of the time response of a given system. As the possible variation of transistor parameters was considered, it followed that a study of all possible roots of the topology equation for the subject phase-shift oscillator was required. This suggested a plotting of the root loci of topology equations generated by various network configurations.

The topology equation for any active network of general configuration of Fig. 4-4 was stated as equation (9).

$$f_1(sCR) + \left(\frac{h_{ie}}{R}\right) f_2(sCR) + h_{fe} = 0 \qquad (9)$$

or when expanded in general

$$\left[a_n s^n + \frac{a_{n-1}s^{n-1}}{CR} + \frac{a_{n-2}s^{n-2}}{(CR)^2} + \cdots + \frac{a_0 s^0}{(CR)^n}\right]$$

$$\left(\frac{h_{ie}}{R}\right)\left[b_n s^n + \frac{b_{n-1}s^{n-1}}{CR} + \cdots + \frac{b_1 s}{(CR)^{n-1}}\right] + h_{fe}s^n = 0 \qquad (11)$$

where n = number of sections in network.

(11) can be manipulated to

$$1 + \frac{h_{fe}s^n/[1 + n(h_{ie}/R)]}{1 + \dfrac{n(h_{ie}/R)s(s + q_1/CR)(s + q_2/CR) \cdots (s + q_{n-1}/CR)}{(s + p_1/CR)(s + p_2/CR)(s + p_3/CR) \cdots (s + p_n/CR)}} = 0 \qquad (12)$$

The first plot made was the root locus for the topology equation representating the passive network:

$$\frac{n(h_{ie}/R)s(s + q_1/CR) \cdots}{(s + p_1/CR)(s + p_2/CR) \cdots} = -1 = 1\epsilon^{\pm jm\pi} \qquad (13)$$

$$m = 1,3,5 \cdots$$

which was of the form to plot the root locus by Evan's method.[24,29] This was plotted for n = 4 and n = 3 as shown in Fig, 4-11 and Fig. 4-13. Note that the root locus for a passive network can be only on the negative real, $\sigma(CR)$, axis.

The roots for the passive network were determined by assuming reasonable values of $(h_{ie}/R)$. These roots became the poles of the active network

$$\frac{ks^n}{(s + r_1)(s + r_2) \ldots (s + r_n)} = -1 \qquad (14)$$

where $k = h_{fe}/\left[1 + n(h_{ie}/R)\right]$

and the root locus of the active network was plotted for $n = 4$ in Fig. 4-10 and Fig. 4-12 and for $n = 3$ in Fig. 4-14. Note that values of $h_{fe}$ determine the roots on the root locus.

F. TIME RESPONSE

The roots can be located by design to produce desired results, specifically, oscillations. If the roots are located in the left hand s plane damping will result. If the roots are exactly on the imaginary $j\omega(RC)$ axis, sustained oscillations will result, at least in theory. If the roots are in the right hand plane, the oscillations will be ever increasing for a linear system. However, the non linear action of the transistor serves to limit the divergence of the amplitude. It is the theory of the authors that the frequency of operation will very closely approximate that which is indicated by the location of the roots in the right hand plane.

For example, from Fig. 4-12 for a given value of $h_{fe}$, say 35, the roots take the form

$s = (-\sigma \pm j\omega)(RC)$ in the left hand plane (L.H.P.) and

$s = (+\sigma \pm j\omega)(RC)$ in the right hand plane (R.H.P.).

Roots in the L.H.P. produce decaying oscillations and were ignored.

For $h_{fe} = 35$, a typical value is

$s = ( + 0.5 \pm j\ 0.66)RC$ which simplifies to

$s = ( 0 \pm j\ 0.66)RC$ for non linear limiting, and by the Residue Theorem

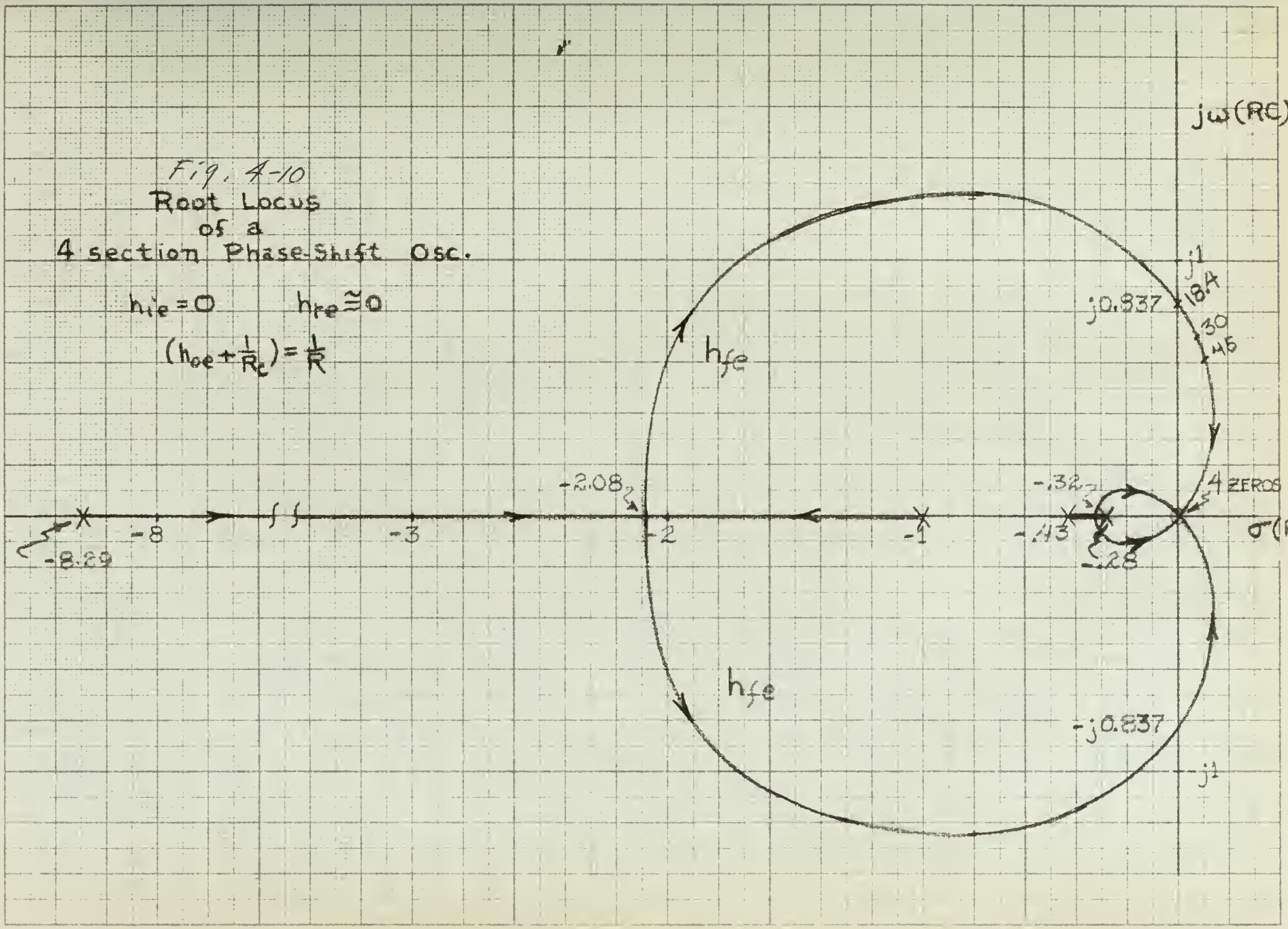


Fig. 4-10
Root Locus
of a
4 section Phase-Shift Osc.

$h_{ie} = 0 \qquad h_{re} \cong 0$

$(h_{oe} + \frac{1}{R_c}) = \frac{1}{R}$

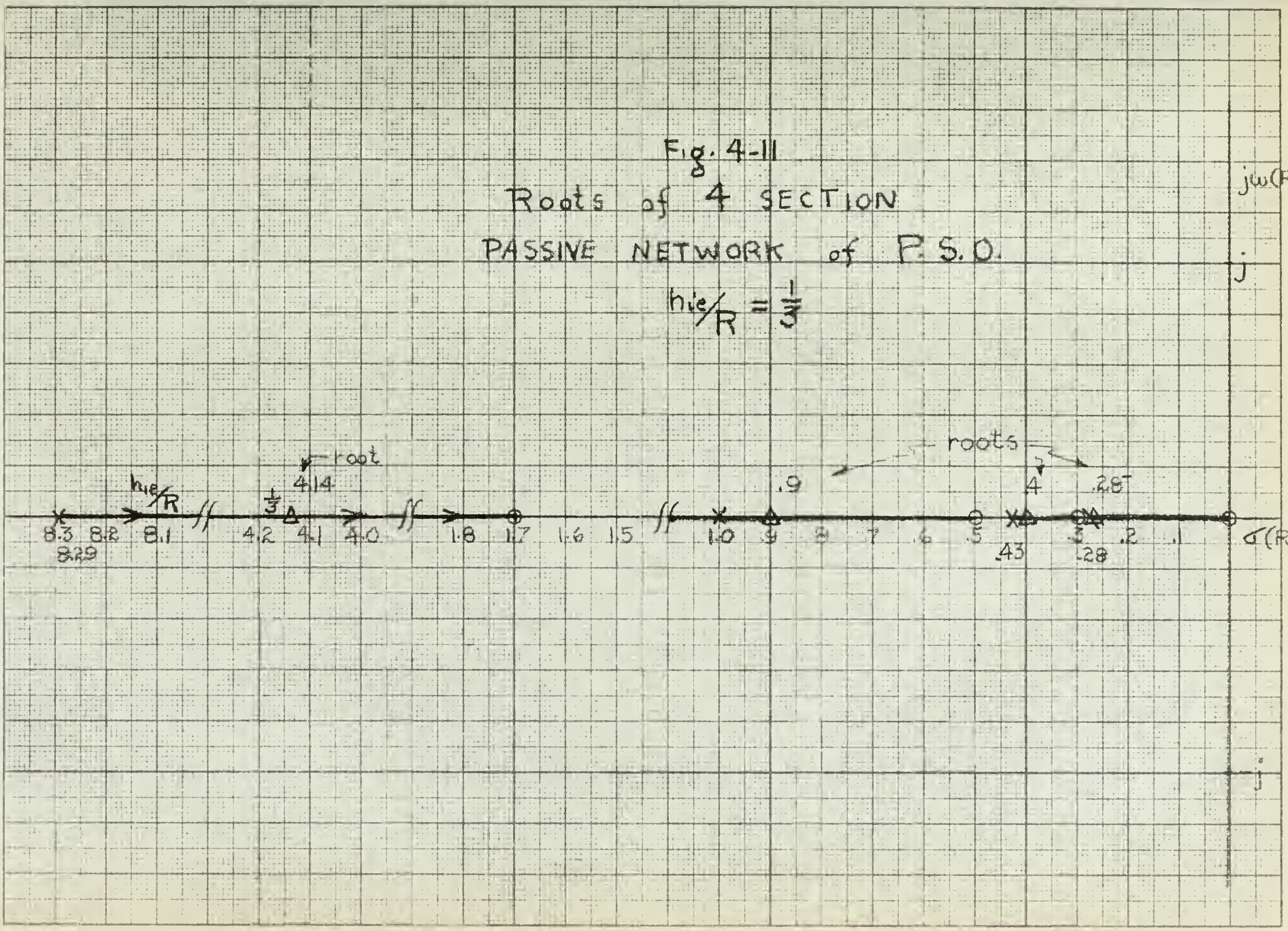


Fig. 4-11

Roots of 4 SECTION PASSIVE NETWORK of P.S.O.

$h_{ie}/R = \frac{1}{3}$

Fig. 4-12

Root Locus

of a

4 section Phase-Shift Oscillator

$h_{ie}/R = 1/3$, $h_{re} \cong 0$

$(h_{oe} + 1/R_C) = 1/R$

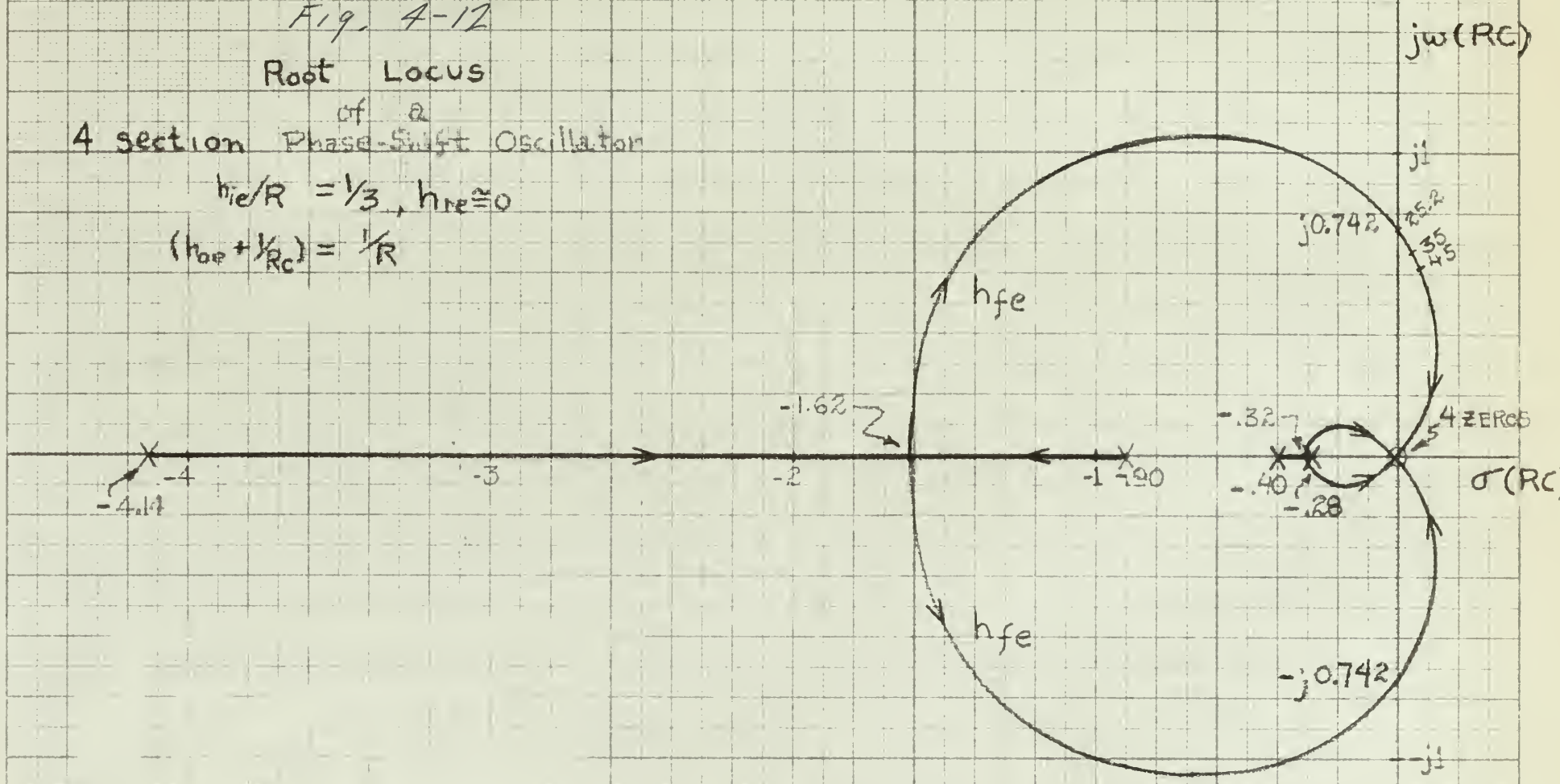

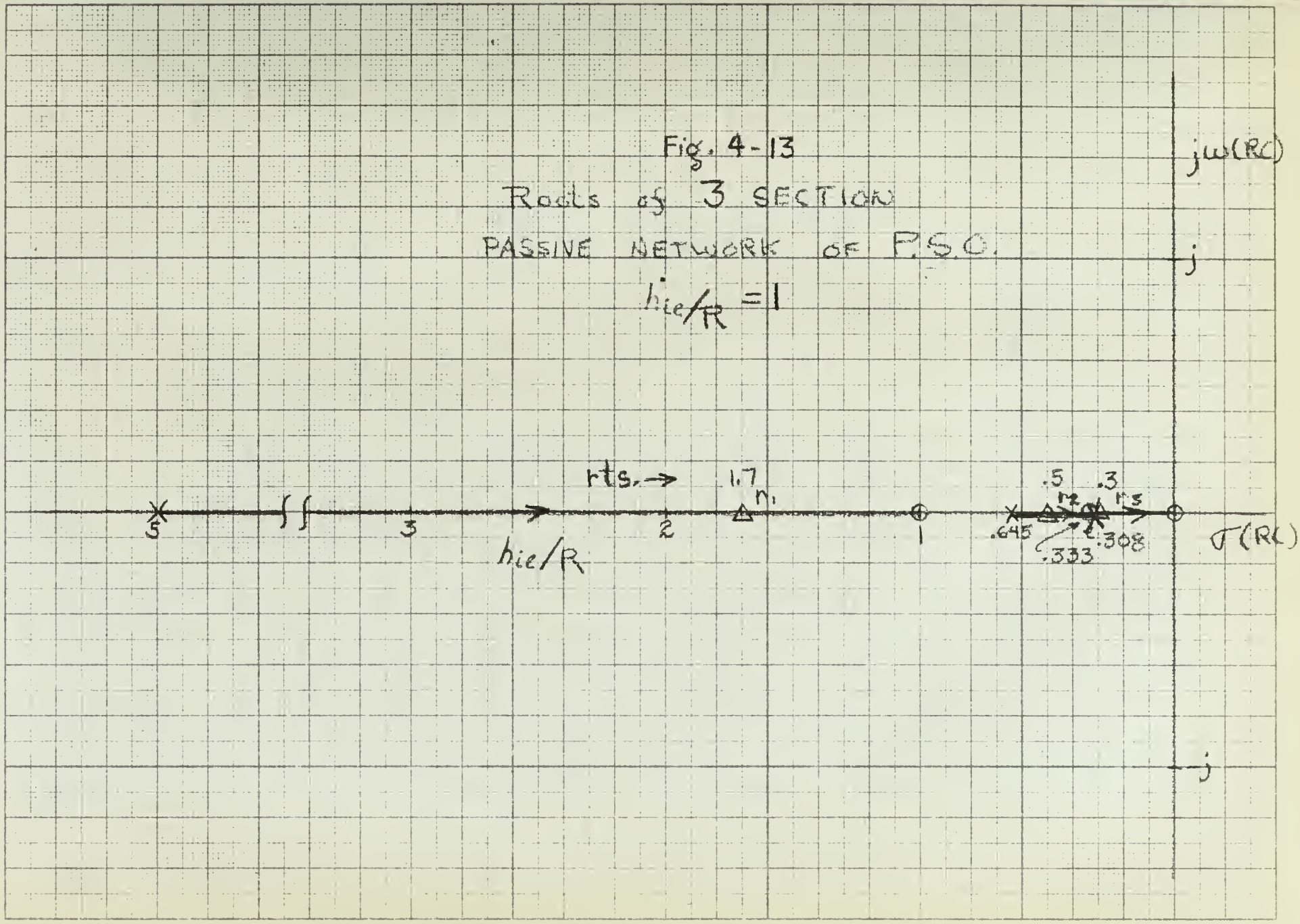


Fig. 4-13

Roots of 3 SECTION PASSIVE NETWORK OF P.S.O.

$h_{ie}/R = 1$

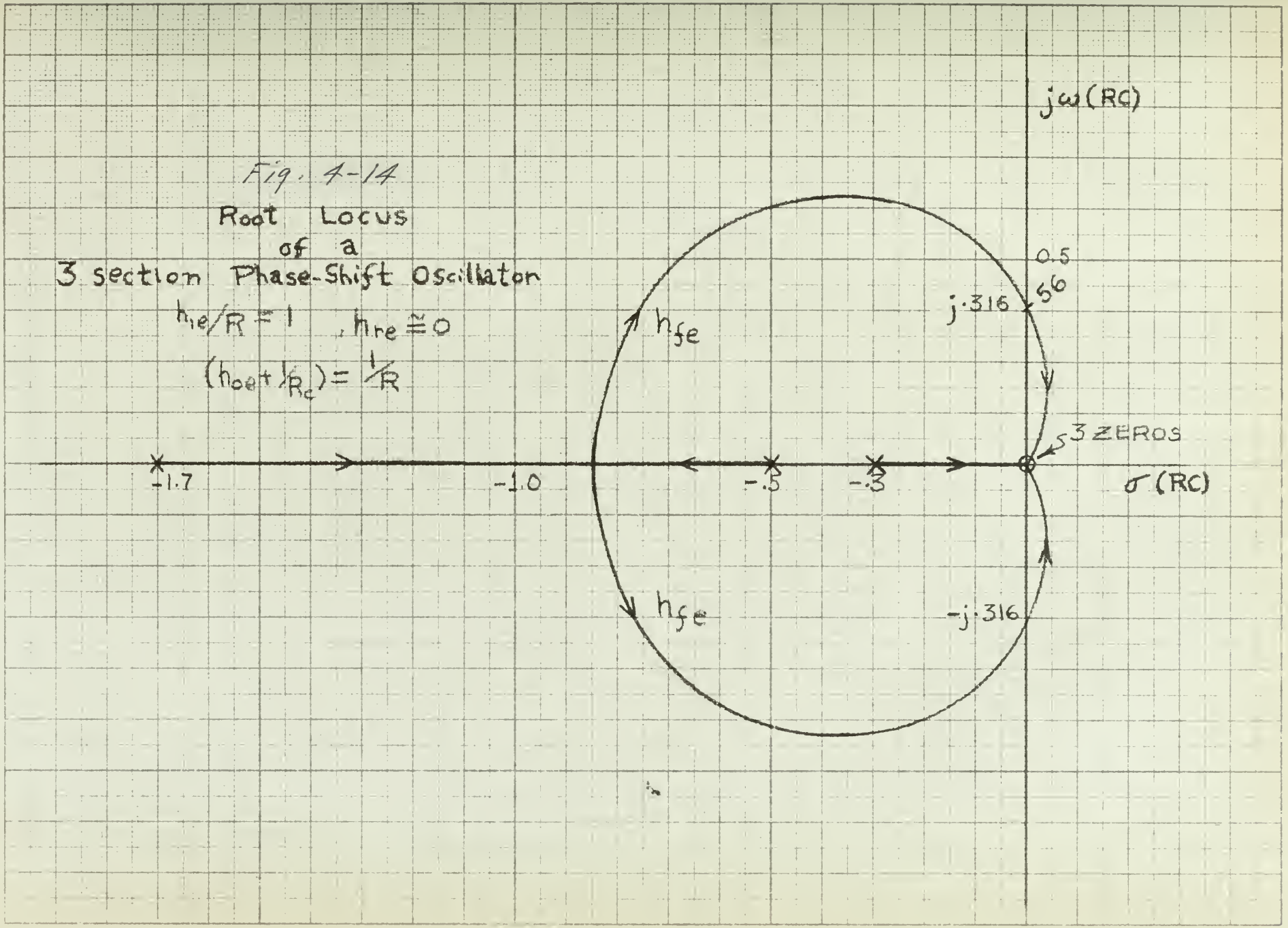


*Fig. 4-14*

Root Locus
of a
3 section Phase-Shift Oscillator

$h_{ie}/R = 1$ , $h_{re} \cong 0$

$(h_{oe} + 1/R_c) = 1/R$

$$f(t)=\left[\sum \text{Residues}\ \frac{e^{st}}{(s+\sigma-j\omega)(s+\sigma+j\omega)}\right]u(t) \quad \text{at roots} \tag{15}$$

$$=\left[\epsilon^{+j\omega t}/2j\omega + \epsilon^{-j\omega t}/-2j\omega\right]u(t)$$

$$= (1/\omega)\sin(\omega t) \tag{16}$$

where $\omega=(0.66)RC$ for this example.

Theoretically, oscillations start as the locus crosses the imaginary axis. This starting point is not only of interest but can be easily found.

On the $j\omega$ axis $\sigma=0$ or $s=\pm j\omega$ (17)

Making substitutions in the topology equation and with $n=4$ and $h_{ie}=0$ in this example

$$(j\omega)^4 + 10(j\omega)^3/RC + 15(j\omega)^2/(RC)^2 + 7(j\omega)/(RC)^3 + 1/(RC)^4$$

$$+h_{fe}(j\omega)^4 = 0 \tag{18}$$

where $j=\sqrt{-1}$

so that

$$\left[\omega^4(1+h_{fe}) - 15\omega^2/(RC)^2\right] + j\left[-10\omega^3 + 7\omega\right] = 0 = 0 - j0 \tag{19}$$

A complex number can vanish only if both the real part and the imaginary part of a given number are zero. Therefore,

$$-10\omega^3/RC + 7\omega/(RC)^3 = 0 \tag{20}$$

$$\omega = (1/RC)\sqrt{7/10}$$

Minimum current gain follows in the same manner.

In general, the starting frequencies are

3 section: $f_{start}=(1/2\pi RC)\sqrt{1/6 + 4(h_{ie}/R)}$

4 section: $f_{start}=(1/2\pi RC)\sqrt{\left[7 + (h_{ie}/R)\right] / \left[10 + 10(h_{ie}/R)\right]}$

which are plotted in Fig. 4-15.

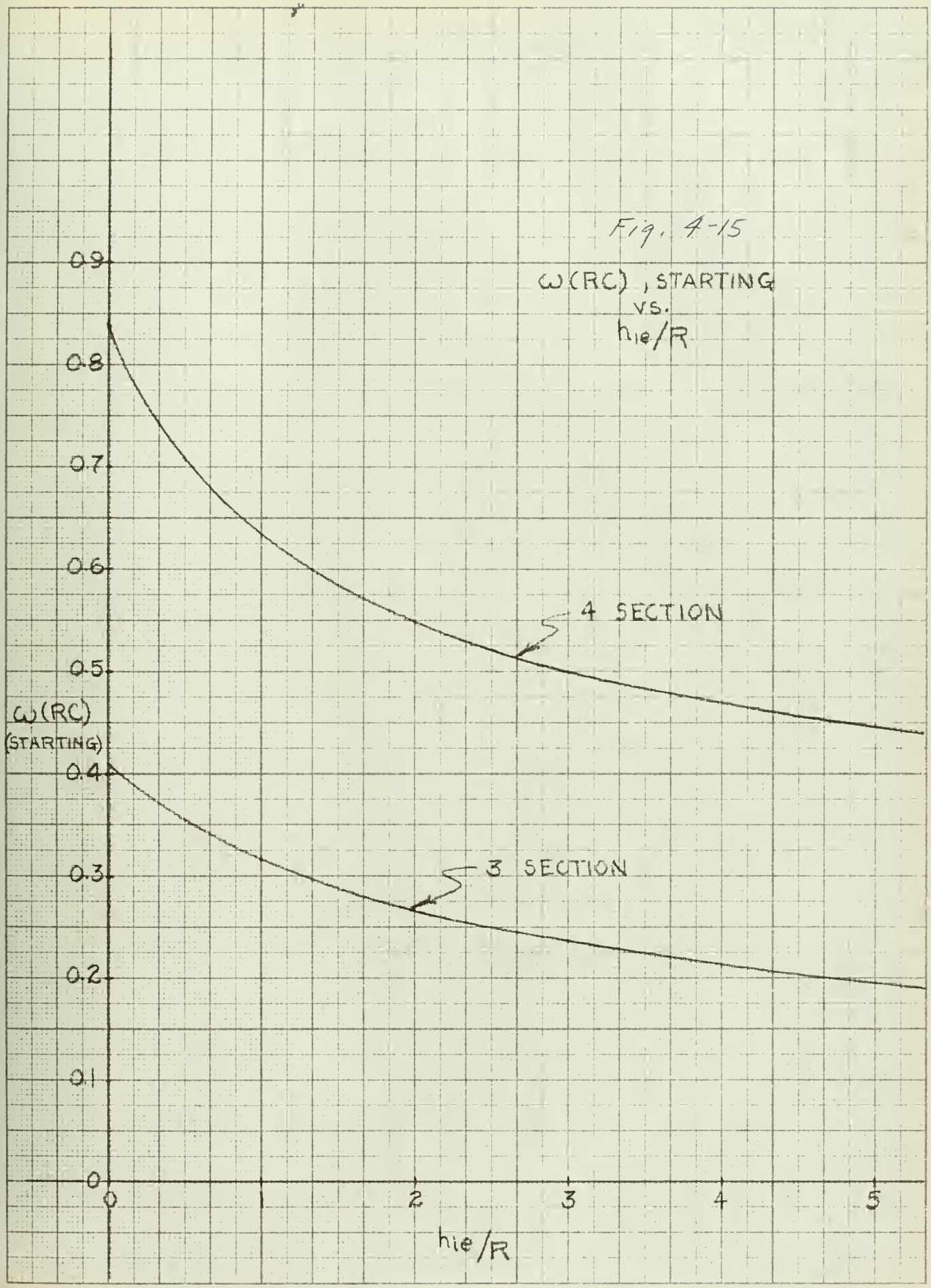
Fig. 4-15
ω(RC), STARTING
vs.
hie/R
0.9
0.8
0.7
0.6
0.5
ω(RC)
(STARTING)
0.4
0.3
0.2
0.1
0
0
1
2
3
4
5
hie/R
4 SECTION
3 SECTION

Minimum current gains for oscillation are

3 section: $4x^2 + 23x + 29 = h_{fe}$

4 section: $$\frac{56x^3 + 473x^2 + 1210x + 901}{x^2 + 14x + 49} = h_{fe}$$

which is plotted in Fig. 4-16

Approximate forms assuming perfect current generator; that is, $h_{ie} = 0$

| Sections | $f_{start}$ | $h_{fe}$ min. |
|---|---|---|
| 3 | 0.065/CR cps | 29.0 |
| 4 | 0.133/CR cps | 18.4 |

G. PREDICTING DERATING OF OSCILLATOR

The locus of roots possible for a four section transistor phase-shift oscillator were plotted on an expanded scale for comparison with experimental results in Fig. 4-17.

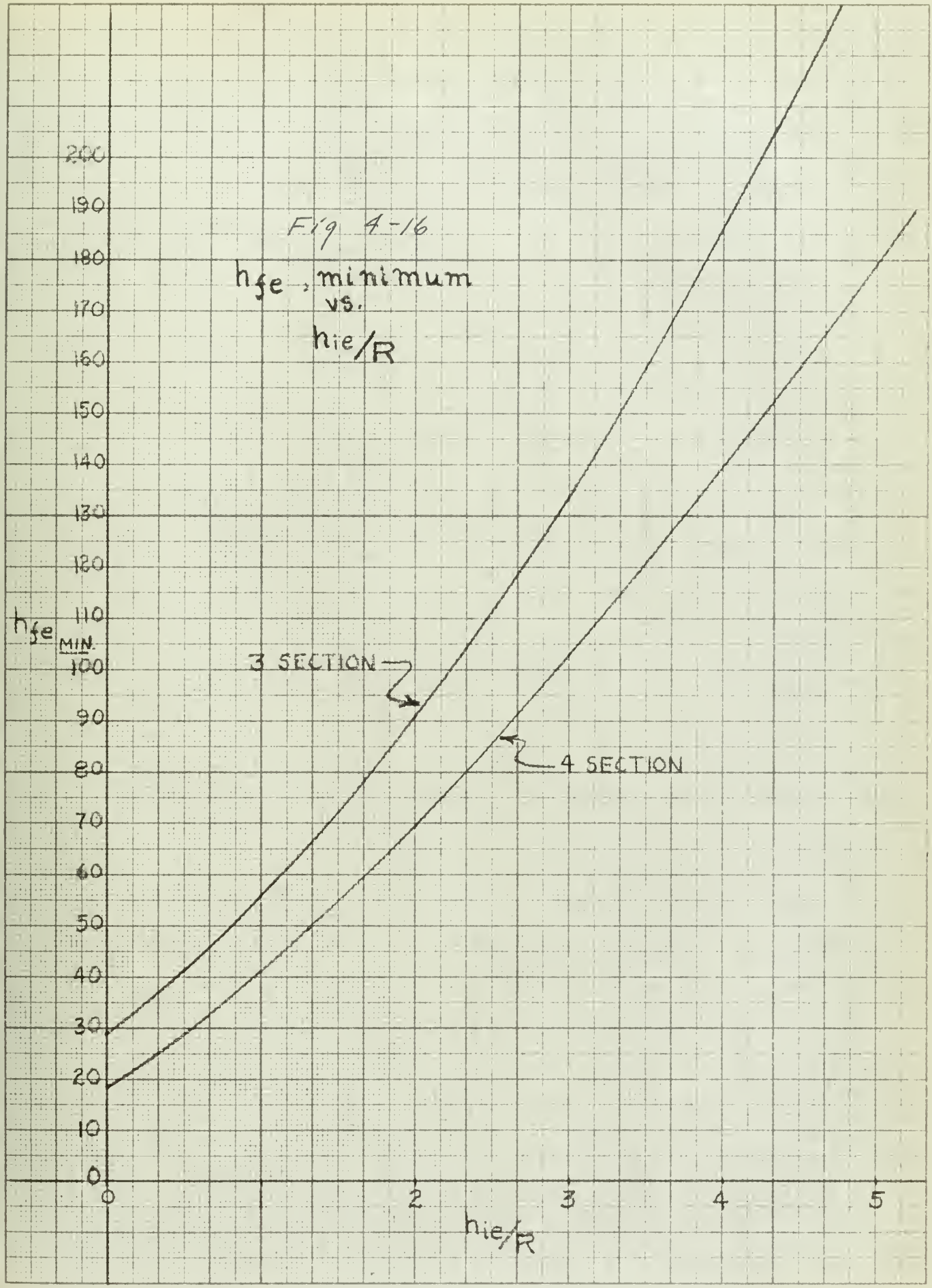
Fig 4-16
$h_{fe}$, minimum
vs.
$h_{ie}/R$
$h_{fe}$ MIN.
200
190
180
170
160
150
140
130
120
110
100
90
80
70
60
50
40
30
20
10
0
3 SECTION
4 SECTION
0
2
3
4
5
$h_{ie}/R$

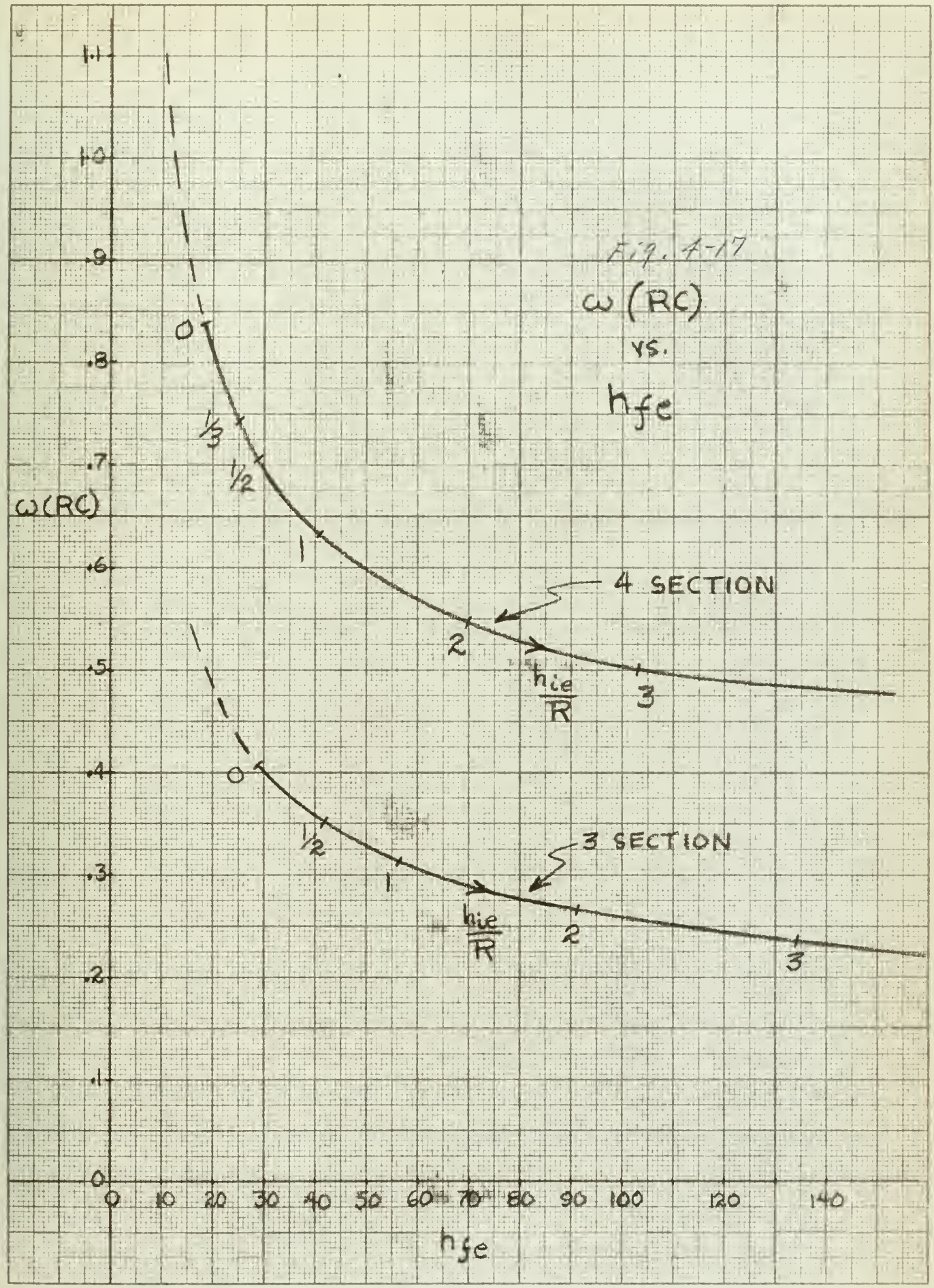
Fig. A-17
ω (RC)
vs.
hfe
ω(RC)
1.1
1.0
.9
.8
.7
.6
.5
.4
.3
.2
.1
0
0
⅓
½
1
2
3
4 SECTION
hie/R
0
½
1
2
3
3 SECTION
hie/R
0 10 20 30 40 50 60 70 80 90 100 120 140
hfe

# CHAPTER 5

## Procedure

### Gamma Source

The test work was performed at the Lockheed Aircraft Company Missiles and Space Division located at Palo Alto, California. The radiation was performed at their 1000 curie cobalt-60 gamma facility. The source was made up from three equal strength cobalt-60 disks spaced equidistantly within a three inch diameter circle. The source was mounted in a long lead slab which could be raised from or lowered into a lead container by means of an overhead hoist.

### Radiation Circuit Board

In order to obtain a uniform flux over all of the oscillator components, the R-C phase shift oscillator shown in Fig. 3-1 was mounted on a three inch diameter fiberglass disk as shown schematically in Fig. 5-1 and as constructed in Fig. 5-2. The disk was mounted in the radiation test jig as pictured in Fig. 5-3. The test jig was constrained to move the oscillator circuit perpendicularly to the face of the gamma source and thereby position the circuit for the desired flux strength.

### Gamma Flux Measurement

Measurement of the gamma ray flux strength at the circuit board was accomplished in the following manner. A blank fiberglass disk was placed in the radiation test jig and the jig was then positioned near the gamma source. After raising the source into position, remote control arms were then used to move the probe of the roentgen rate meter over the back surface of the disk to obtain the average flux reading. All runs were made with the radiation circuit board positioned in an average radiation flux field of $1.7 \times 10^6$ roentgen per hour.

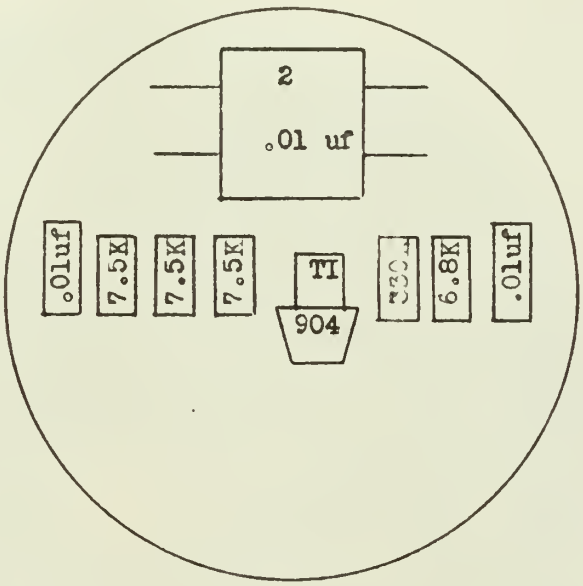


Figure 5-1

Component identification and location

for an R-C phase shift oscillator.

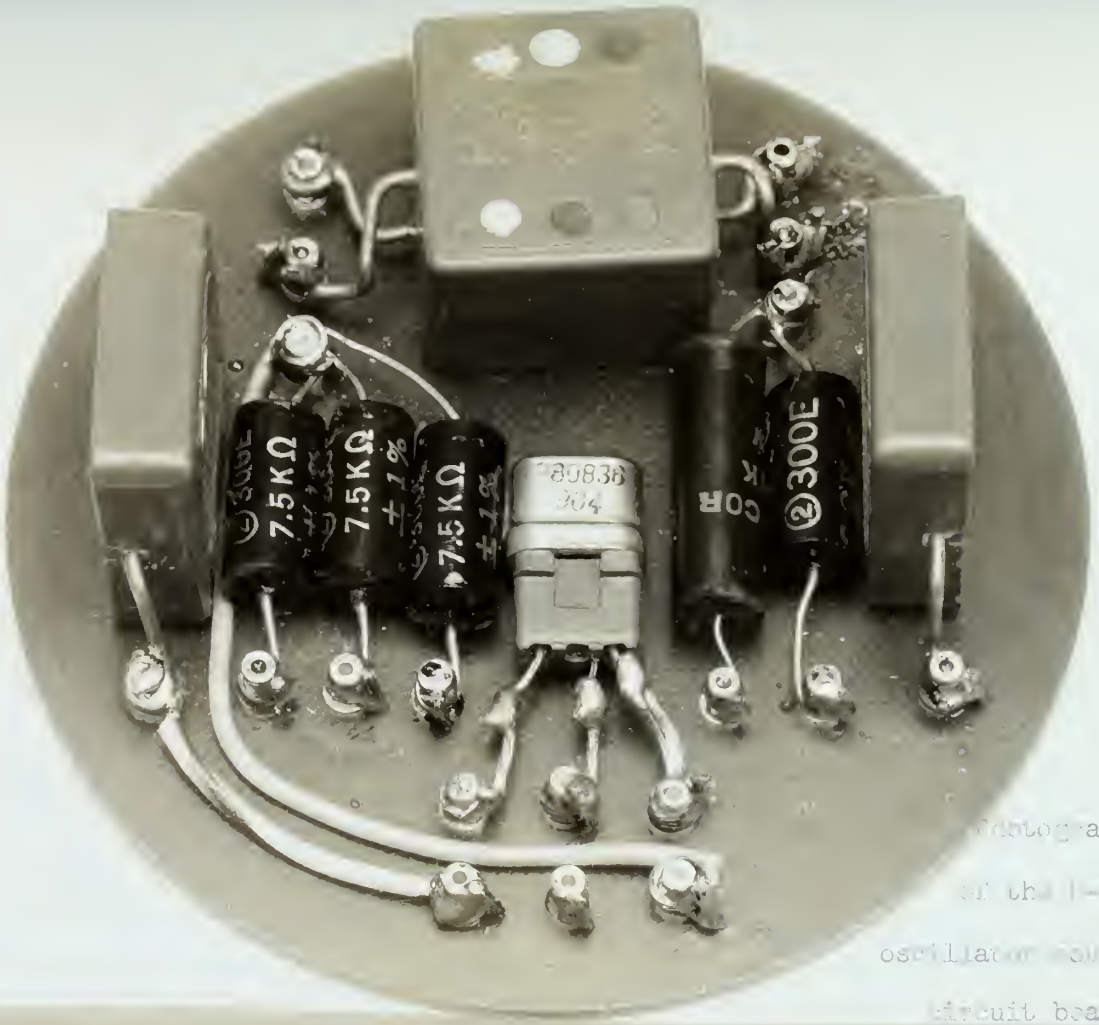


Figure 1-2

Photograph of the components of the R-C phase shift oscillator mounted on the radiator circuit board.

# R-C PHASE-SHIFT OSCILLATOR

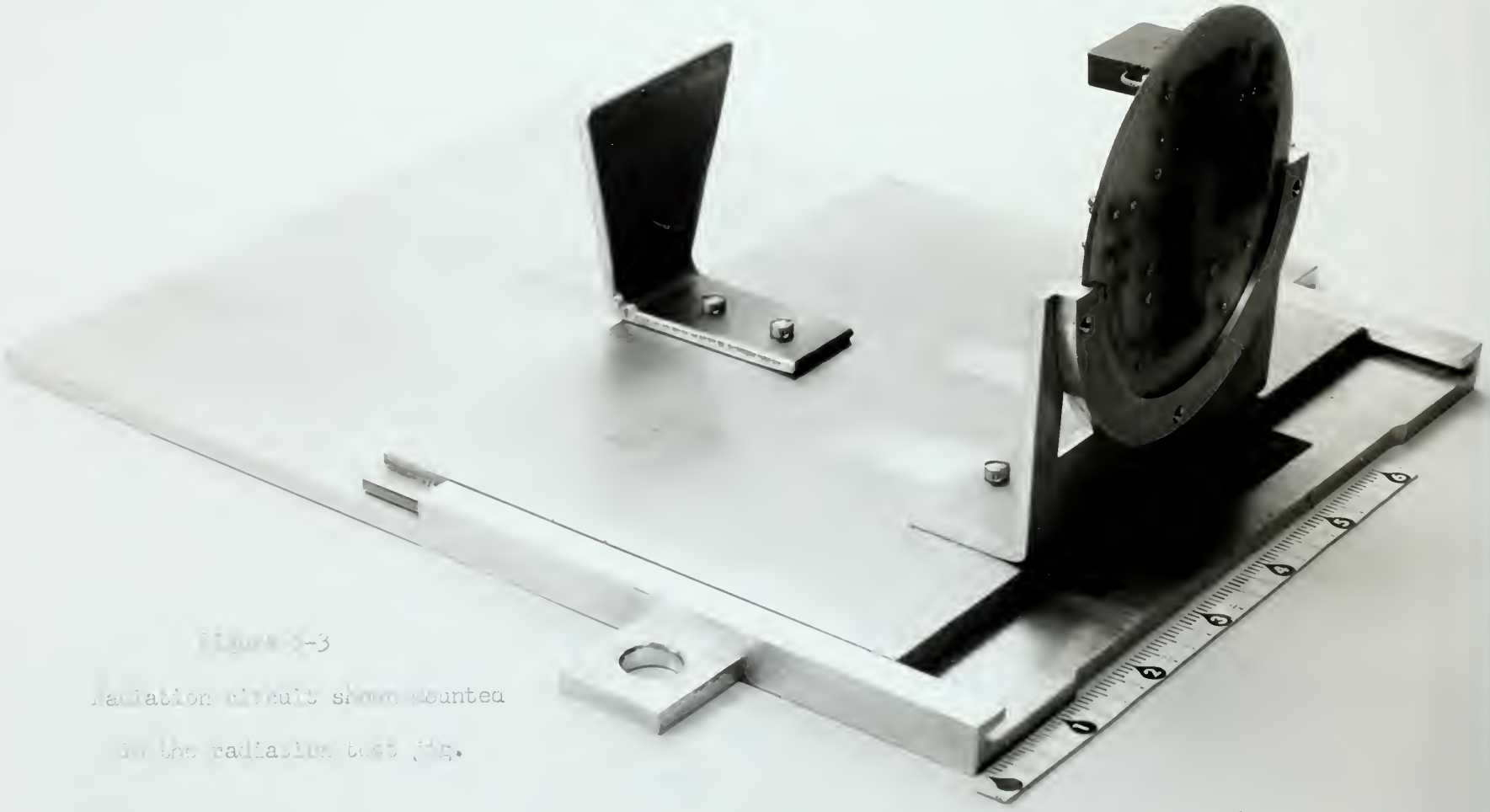

Figure 5-3

Radiation circuit shown mounted

in the radiation test jig.

Oscillator Control Panel

A switching arrangement called the oscillator control panel was constructed in order to run either of two oscillators from the same power source. A wiring schematic of the control panel and associated oscillator circuits is shown in Fig. 5-4 and pictured in Fig. 5-5. The irradiated R-C phase shift oscillator was duplicated at the control panel. This circuit was called the reference oscillator. By means of the control panel, either circuit could be run individually or with any combination of its own or the other circuit's components. The switching arrangement permitted a rapid check of the irradiated circuit in order to determine which component or components had been affected by the gamma flux.

Both circuits could not be run simultaneously by this method. Therefore the switching arrangement provided selected switching of the unused transistor to a transistor test set which was set to match the operating condition of the transistor in the irradiated circuit.

Instrumentation

Fig. 5-6 is a block diagram of the instrumentation used to monitor the radiation runs. Prior to irradiating each circuit, the output frequency and output voltage were recorded for the following oscillator circuit configurations:

1. Circuit to be irradiated operating.
2. Reference circuit operating.
3. Circuit to be irradiated operating on reference transistor.
4. Reference circuit operating with all components of circuit to be irradiated switched in individually.

This information later provided a quick and logical check on the

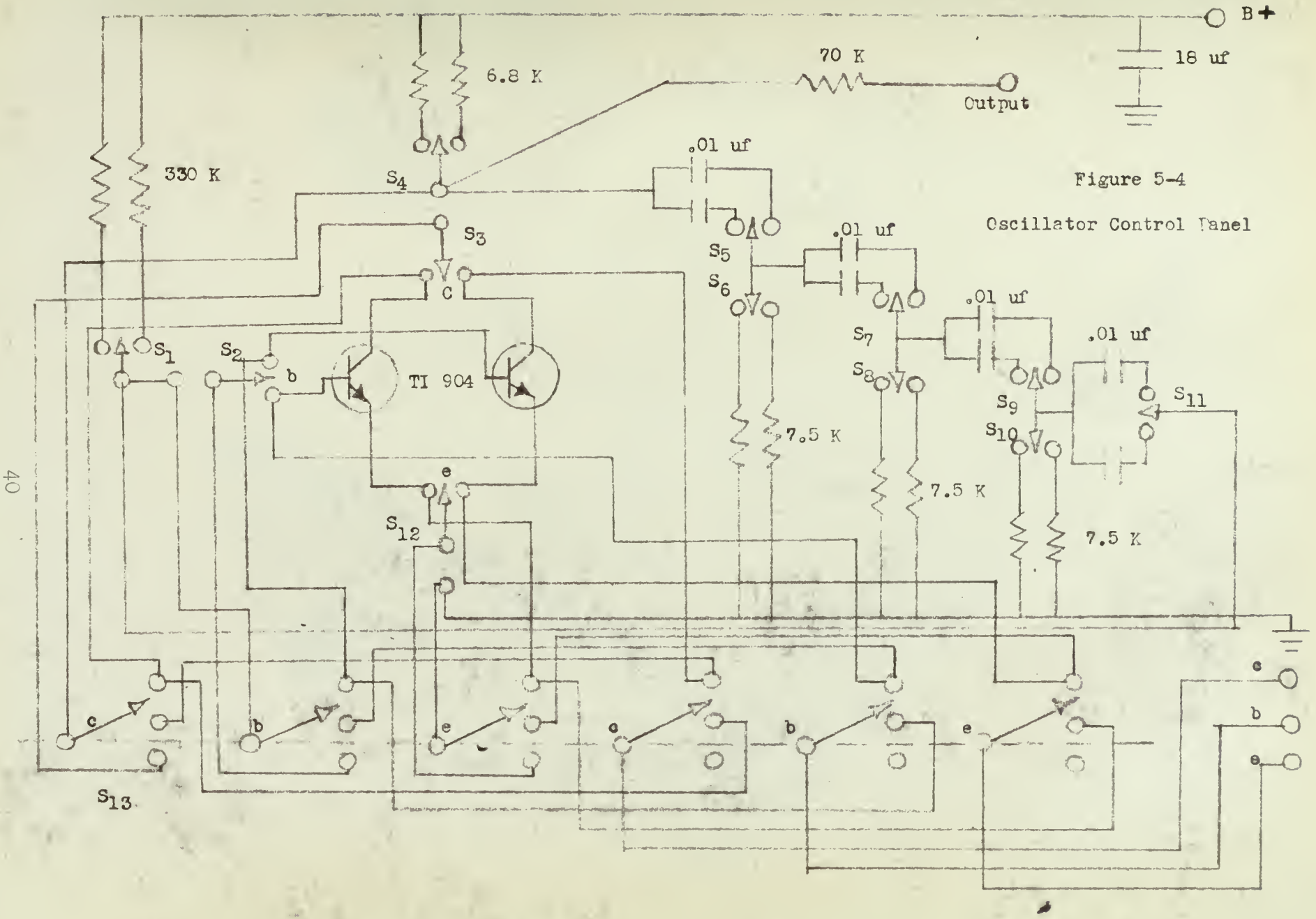


Figure 5-4

Oscillator Control Panel


OSCILLATOR CONTROL PANEL
Black Test
Red Ckt
Red Test
Black Ckt
MAN.
SWITCH
6.3K
7.5K
7.5K
330K

Figure 5-6

Measurements Block Diagram

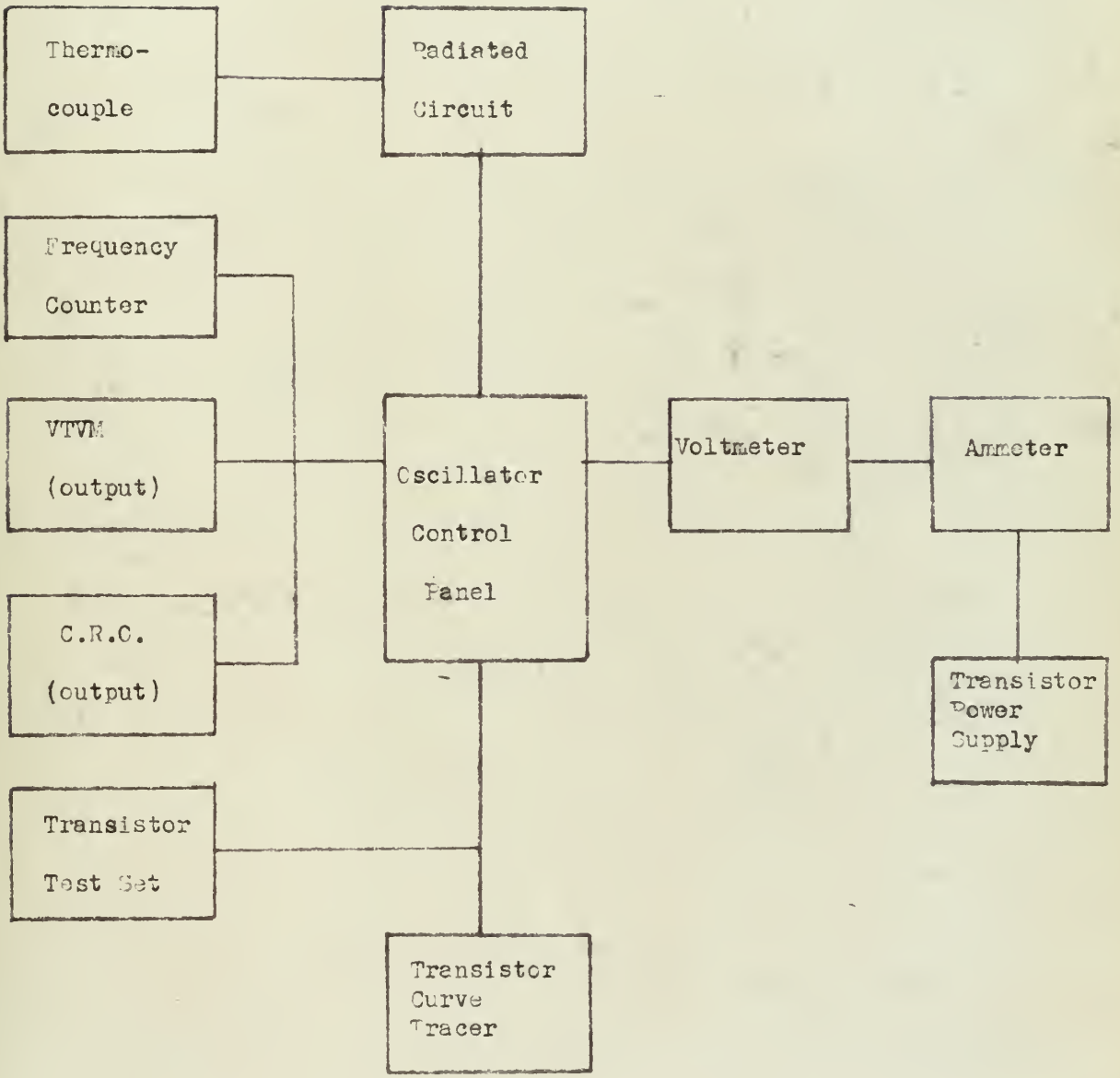

irradiated circuit. Since any change in the components was immediately reflected by a change in the output frequency of a phase shift oscillator, frequency shifting was the primary gage used to detect changes in the irradiated components. The transistor was expected to be the most sensitive component in the irradiated circuit. Therefore the first check made on noting an output frequency shift was to interchange the reference transistor with the one undergoing irradiation. If the new frequency obtained was not the same as originally recorded, the components were checked individually with the original frequencies recorded in 3. above. In this manner, the components which had changed their parameters in the gamma flux would be identified.

As stated previously, the inactive transistor was always switched to the Owen Bridge transistor test set which was always set to match the operating condition measured in the irradiated oscillator circuit. This arrangement in addition to permitting measurement of the transistor parameters prevented temperature change effects on the transistor switched to the test set as well as preventing the introduction of a cold transistor to the reference circuit whenever that particular circuit was called upon to operate.

Considerable difficulty was experienced in obtaining identical readings of the hybrid, "h", parameters for the same transistor when it was physically on the transistor test set as well as when it was switched to the test set from the radiation circuit board through some 20 feet of wiring. A small capacitor to ground was used as a probe and it was determined that the capacitive effect on the collector wiring was the cause of the difference in the readings. The unshielded collector wire was replaced by RG 62/U coaxial cable and the transistor parameter readings made remote-

ly were found to agree with the readings obtained for the same transistor physically on the transistor test set. The circuitry for measuring the various hybrid transistor parameters is presented in Fig. 5-7 and Fig. 5-8.

Figure 5-7

Circuits used in measuring the hybrid transistor parameters as found in the Owen Laboratories' Type 210-A Transistor Test Set.

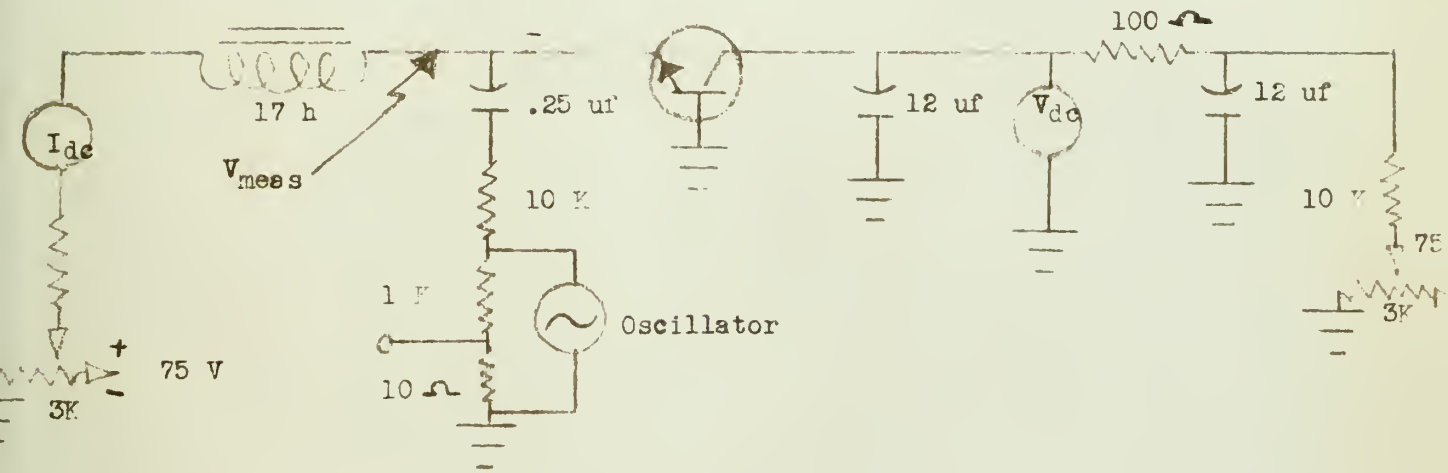


(a) Circuit used to measure input impedance, $h_{ib}$.

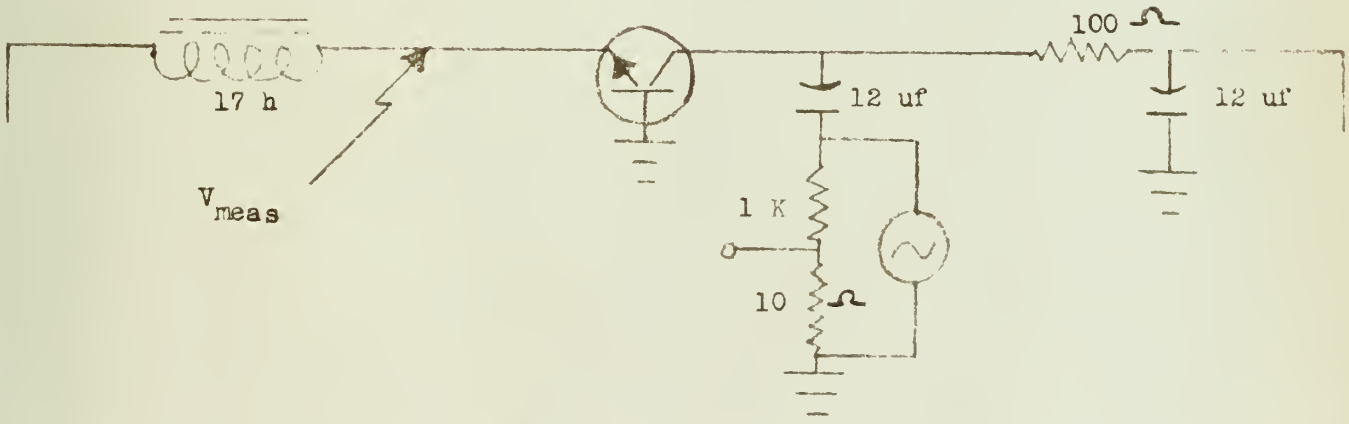


(b) Circuit (a) modified in order to measure feedback voltage ratio, $h_{rb}$.

Figure 5-8

Circuits used in measuring the hybrid transistor parameters as found in the Owen Laboratories' Type 210-A Transistor Test Set. The circuits are modifications of the circuit in Fig. 5-7 (a).

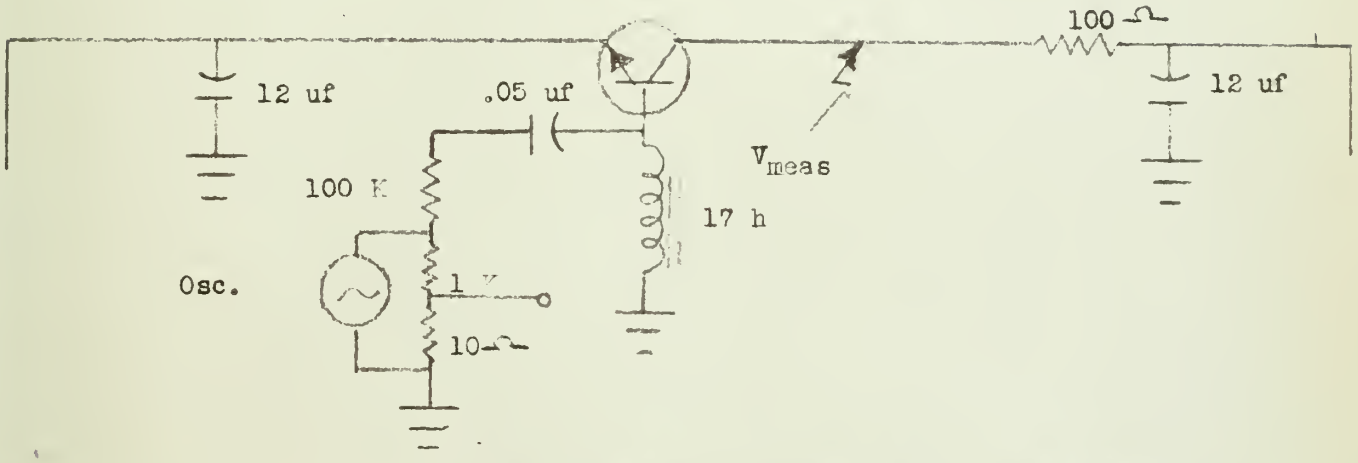


(a) Circuit to measure small signal current gein, $h_{fe}$.

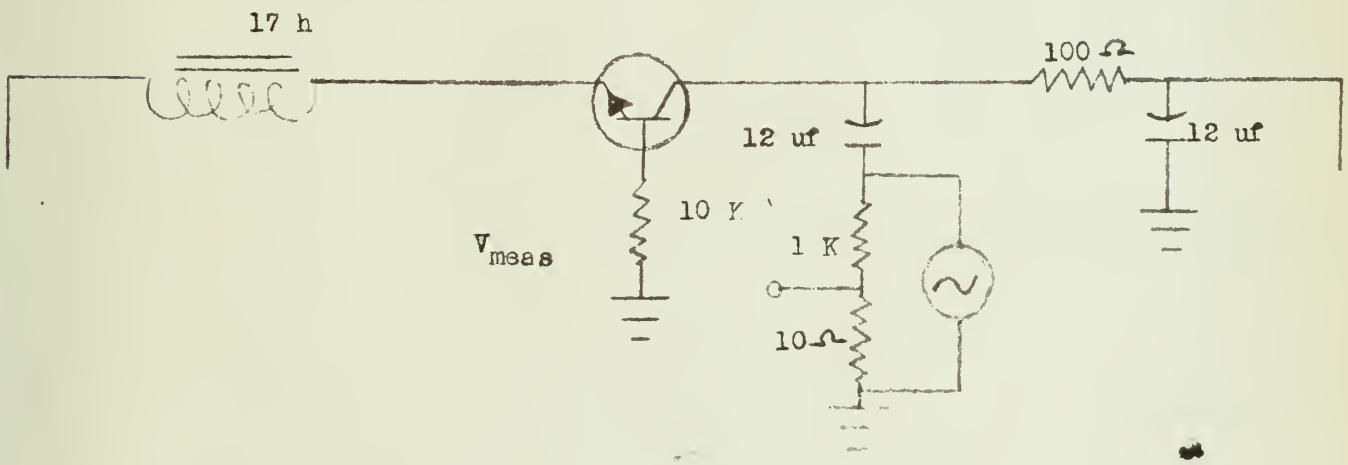


(b) Circuit to measure output admittance, $h_{ob}$.

CHAPTER 6

## Results and Discussion

The following measurements were recorded:

a. Dose----roentgen/hour.

b. Temperature, $^{o}C$

c. Supply voltage, $V_i$

d. Emitter current, $I_e$

e. Collector voltage, $V_c$

f. Output voltage, $V_o$

g. Output frequency, f

h. Transistor forward current gain, $h_{fe}$

i. Transistor output admittance, $h_{ob}$

j. Transistor feedback voltage ratio, $h_{rb}$

k. Transistor input impedance, $h_{ib}$

A total of seven circuits were irradiated in a mean flux of $1.7 \times 10^{6}$ roentgen per hour. Four runs were carried on until the ultimate failure of the circuit. Three runs were continued only so long as deemed necessary to provide or substantiate the characteristic trends for the various parameters recorded.

The operating point for each circuit was the one at which the following conditions were met:

a. The circuit to be irradiated must have operated with the reference transistor switched in.

b. The reference circuit must have operated.

c. The reference circuit must have operated with each component from the circuit to be irradiated switched in individually.

For the conditions imposed, the optimum operating voltage was found to be approximately 15 volts.

The output frequency and output voltage measurements were considered to be raw data in that no compensation was made for the stray wiring capacitance. It is to be stressed, however, that these were none-the-less representative readings and accurately portray the trends of these parameters in the influence of a radiation field. The transistor parameters, on the other hand, were considered correct in that coaxial cable was used in connecting the transistor to the control panel.

The plots of $h_{ib}$, $h_{rb}$, $h_{ob}$, $h_{fe}$, $V_o$, and f as a function of dosage are presented in Fig. 6-1 through Fig. 6-6 respectively. The following tabulation shows those runs which deviated from the general trend for each parameter measured.

| Parameter | Deviate Curves |
|---|---|
| $h_{ob}$ | 3,5,6* |
| $h_{rb}$ | 4,5,6 |
| $h_{ib}$ | 4,5,6 |
| $h_{fe}$ | 4,5 |
| $V_o$ | 4,5* |
| f | 4,5* |

*Run seven was neglected because insufficient points were taken in these cases.

From each family of curves a representative mean curve could have been constructed having the following characteristics:

a. $h_{ob}$ was essentially a constant at $.6 \times 10^{-6}$ mhos with a slight increase in value noted as the circuit failed.

b. $h_{rb}$ was essentially a constant at its initial value with a

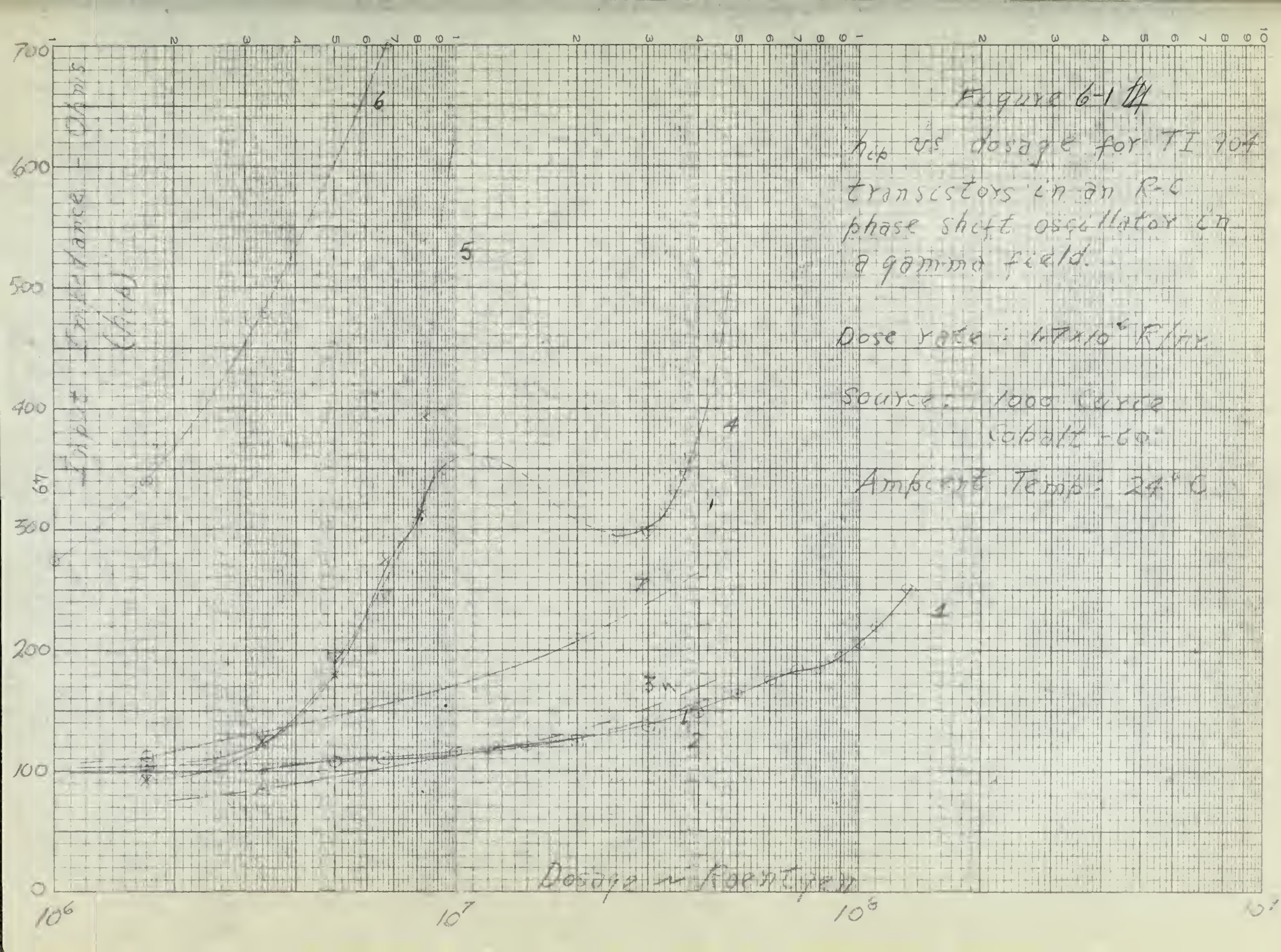
Figure 6-14
$h_{fe}$ vs dosage for TI 904 transistors in an R-C phase shift oscillator in a gamma field.
Dose rate: $1.7 \times 10^4$ R/hr
Source: 1000 curie cobalt-60
Ambient Temp: 24° C
Transistance (G-A)
Dosage — (rads)
700
600
500
400
300
200
100
0
$10^6$
$10^7$
$10^8$
$10^9$
1
2
3
4
5
6
7

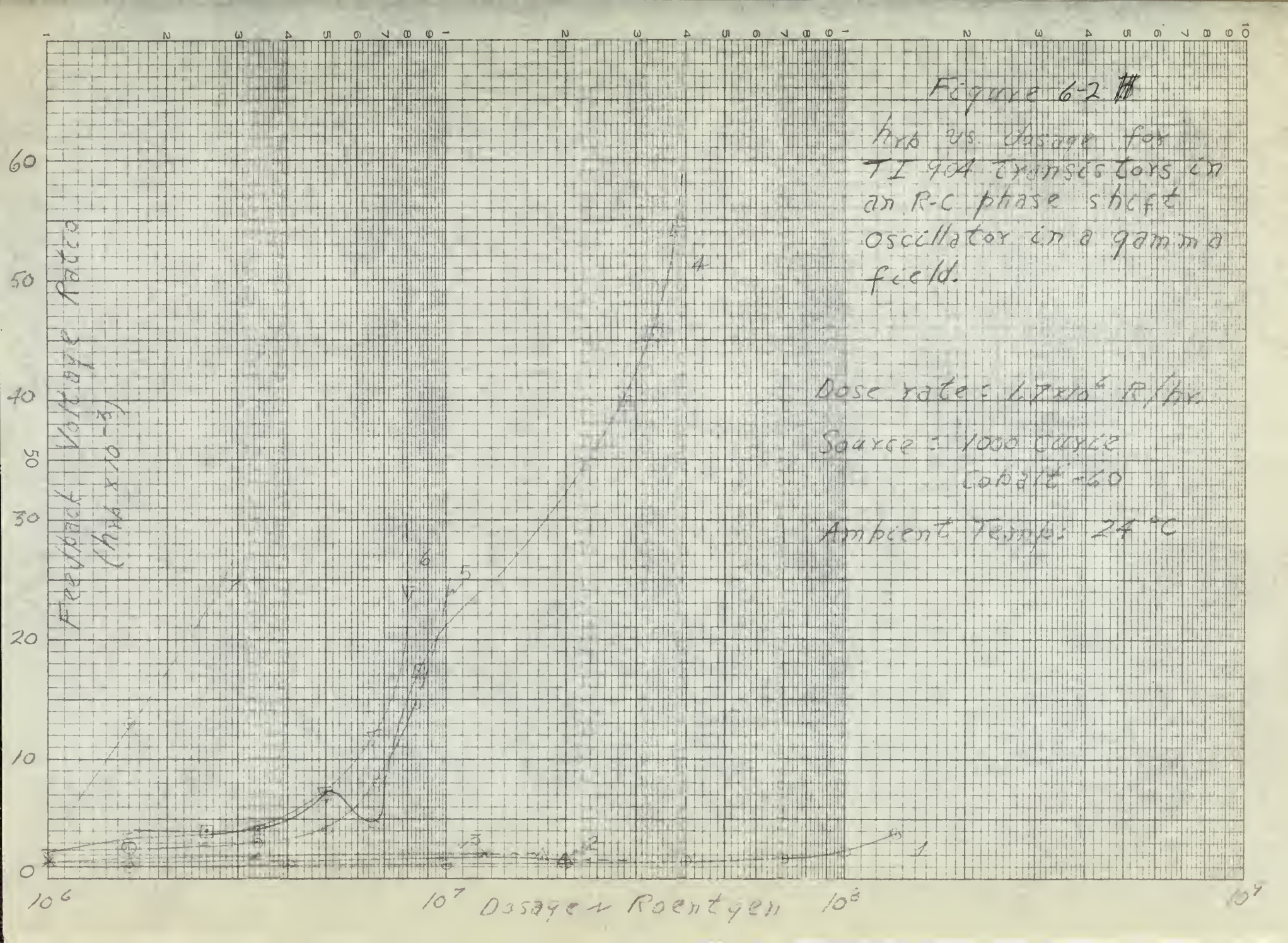
Figure 6-2
hFE vs dosage for TI 904 transistors in an R-C phase shift oscillator in a gamma field.
Dose rate: 1.2x10^6 R/hr.
Source: 1000 Curie Cobalt-60
Ambient Temp: 24 °C
Feedback Voltage Ratio (hFE x 10^-3)
60
50
40
30
20
10
0
10^6
10^7 Dosage Roentgen
10^8
10^7

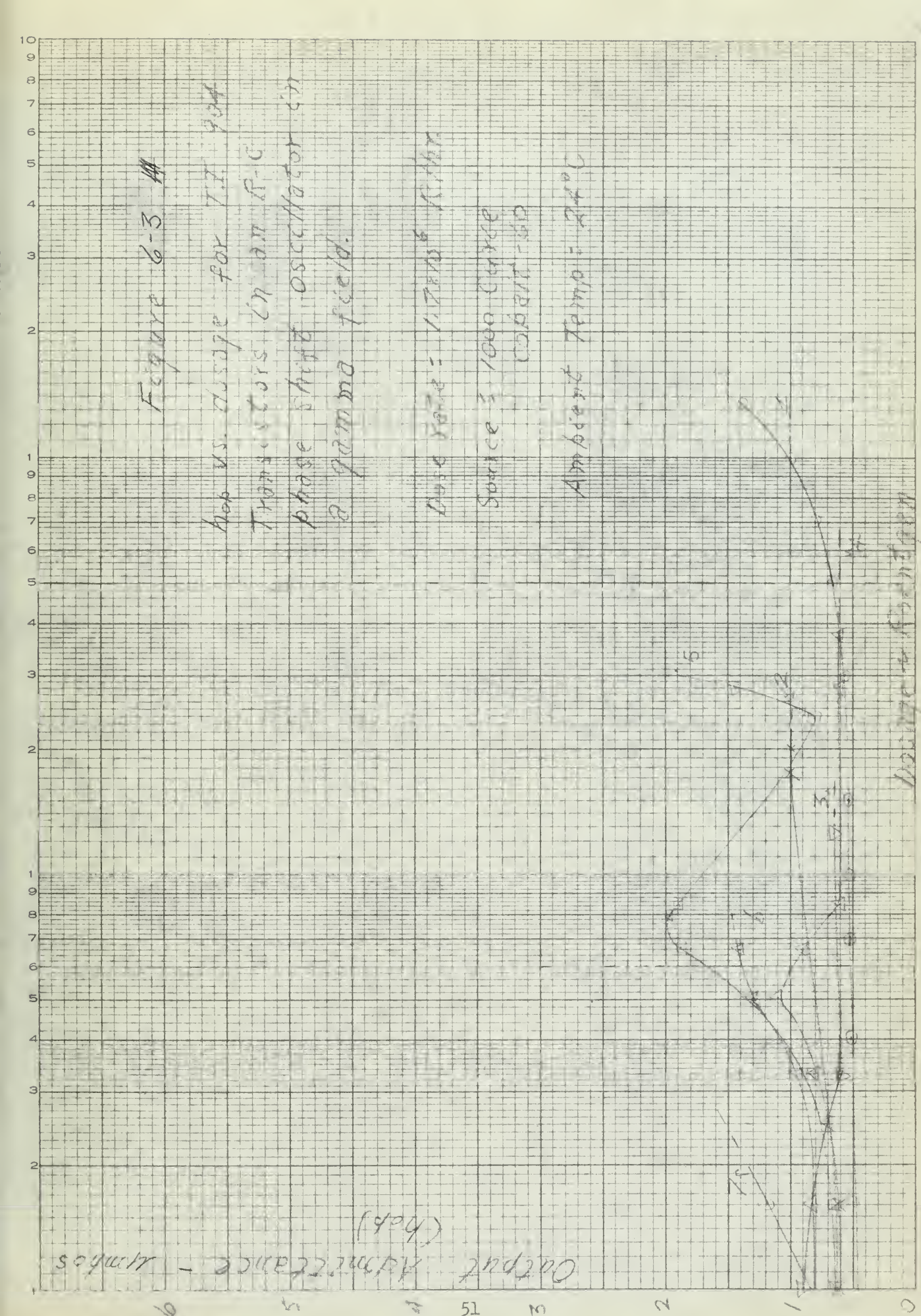
Figure 6-3
log versus square root of frequency
Transistor Common Emitter Output Admittance - Mhos
Phase shift oscillator
2 gain fields
Date Mar. 1960
Source 1000 Cycle
Ambient Temp. 25°C
Output Admittance (Mhos)
Square Root of Frequency (KC)

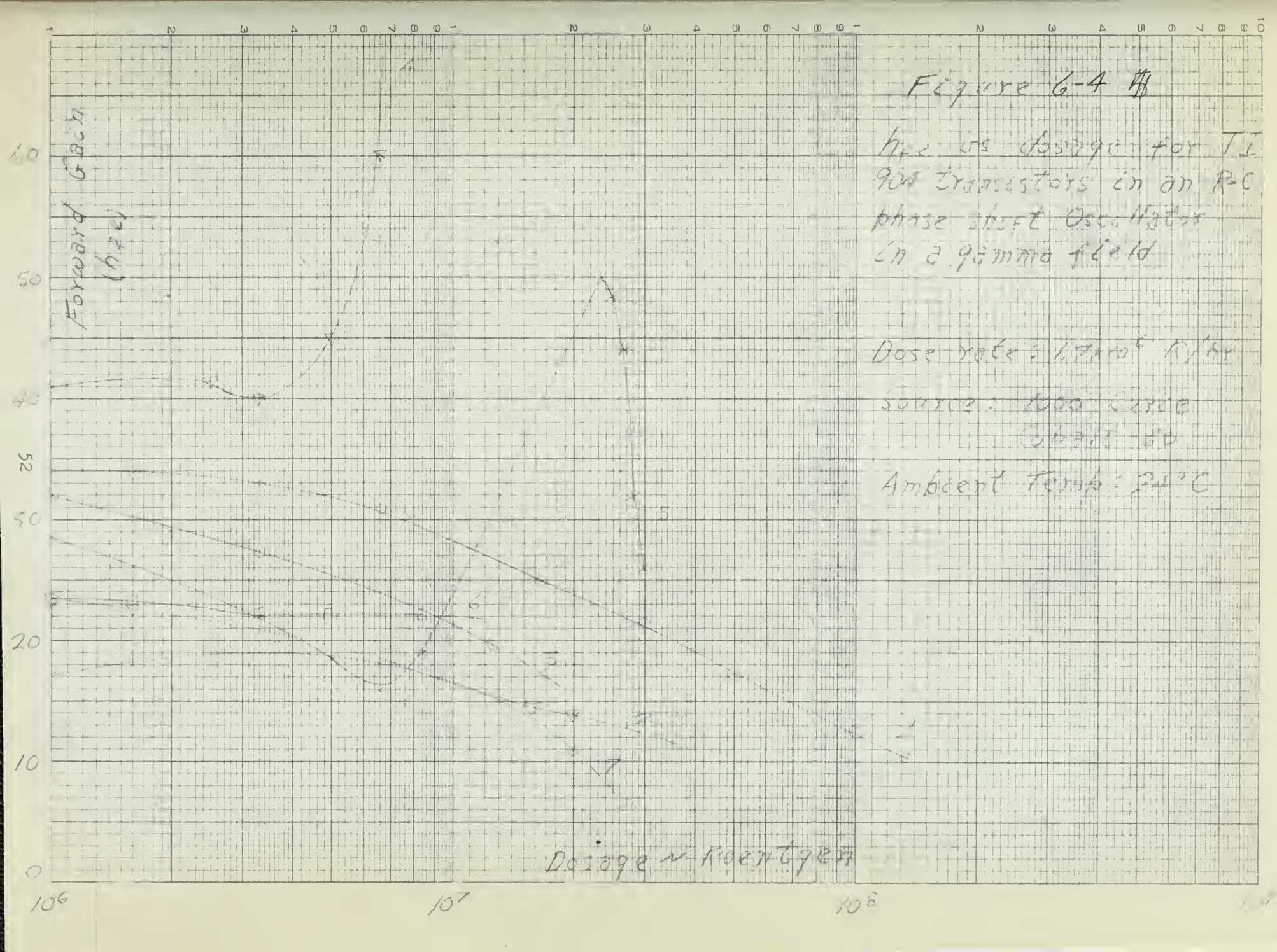
Figure 6-4
Dosage - Rad (Si)
Change in hFE
10
20
30
40
50
52
0
10^6
10^7
10^8

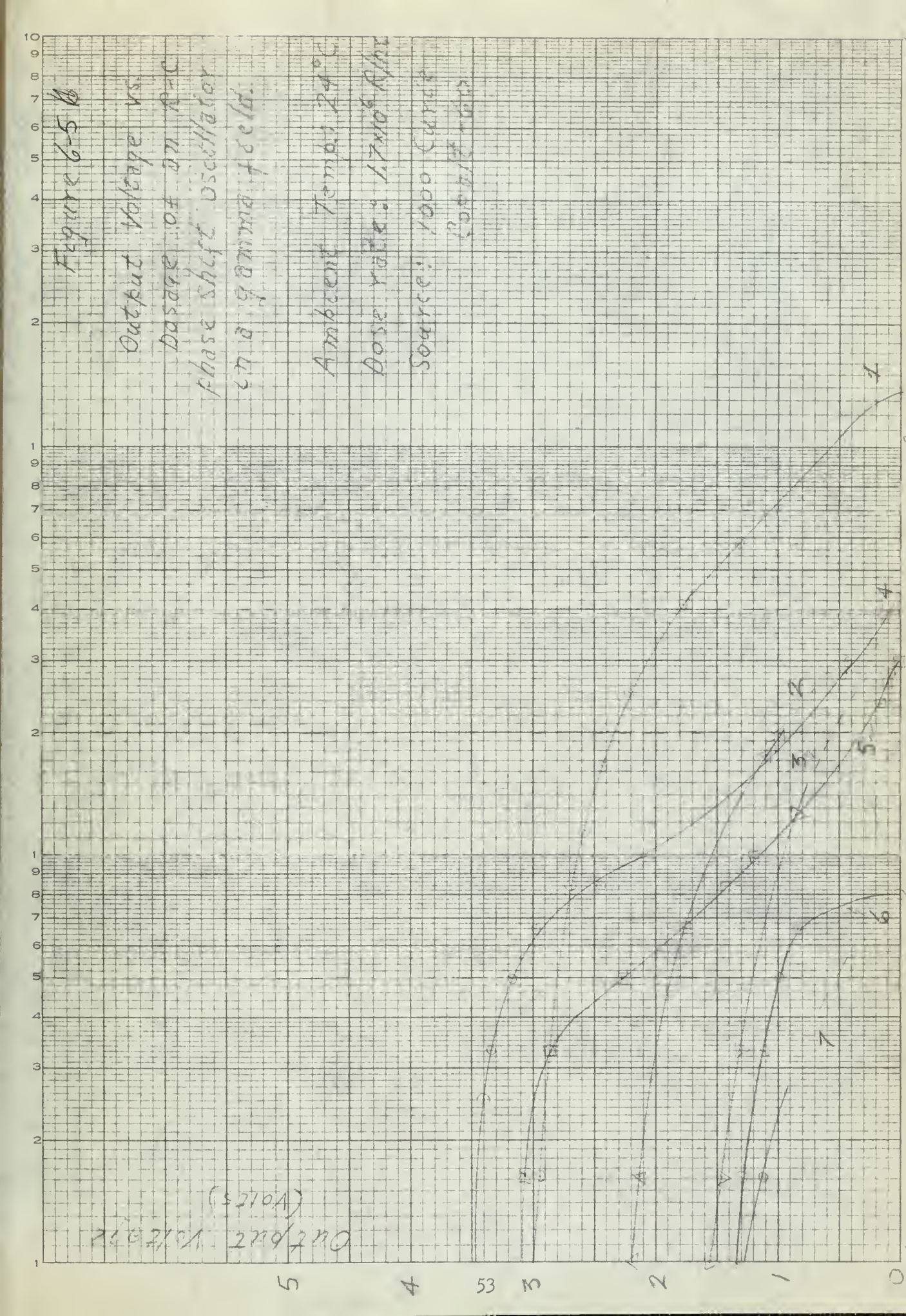
Figure 6-5
Output voltage vs.
base of 2N1711
phase shift oscillator
with a 5 ohm load.
Ambient temp. 24°C
Base width: 1.7x10⁻⁴ cm
Source: 100 curies Co⁶⁰
Dosage-rate (rads/min)
Dosage (rads)
(5270A)

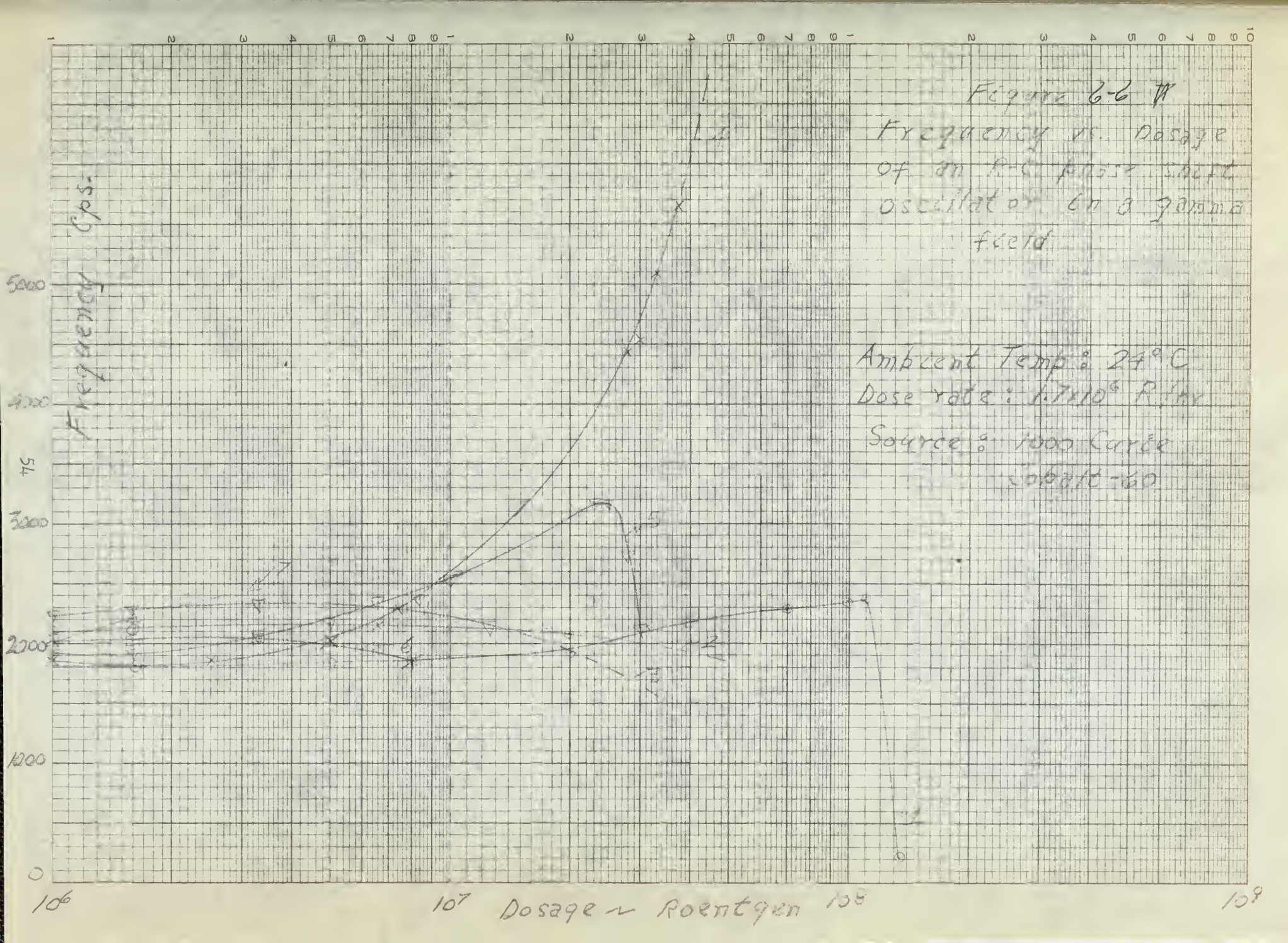
Figure 6-6 M
Frequency vs. Dosage
of an R-C phase shift
oscillator in a gamma
field
Ambient Temp: 24°C
Dose rate: 1.7x10⁶ R/hr
Source: 1000 Curie
cobalt-60
Frequency (cps)
5000
4000
3000
2000
1000
0
10⁶
10⁷
Dosage ~ Roentgen
10⁸
10⁹

slight increase in value as the circuit failed.

c. $h_{ib}$ exhibited a constant rise in value throughout irradiation.

d. $h_{fe}$ was essentially a constant until reaching a total dose of $3x10^6$ roentgen after which it showed a constant decrease.

e. $V_o$ exhibited two general decay slopes with the break occuring at a dose of $10^7$ roentgen.

f. Frequency output showed a continual rise with marked peaking near the failure of the circuit with a sudden decrease.

It was noted that in those cases in which the oscillator experienced failure, the oscillations could always be regained by increasing the power supply. The increase in power supply had the effect of raising the operating point of the transistor in the circuit. Indications were that the oscillations could be sustained in this manner until the transistor was damaged to the extent that its forward current gain would be below that required for circuit oscillation.

The transistor was the only affected component in all cases. No changes were observed in the resistors or capacitors. It becomes apparent that any shielding to be used with this type of oscillator should be used about the transistor only.

Fig. 6-7 and Fig. 6-8 are failure analysis curves for the TI 904 transistor. The behavior of the forward current gain, $h_{fe}$, was the most significant parameter of the transistor which influenced circuit operation. Fig. 6-7 and Fig. 6-8 express the probability of failure for the derating of $h_{fe}$ as a function of gamma dosage.

Fig. 6-9 through Fig. 6-12 are the failure analysis curves for the circuit. They express the probability of failure for the derating of the

output voltage, $V_o$, as a function of gamma dosage and the probability of failure for the derating of the output frequency as a function of gamma dosage.

The failure analysis curves were constructed in the following manner. The information, $h_{fe}$, $V_o$, and f as functions of gamma dosage, from Fig. 6-4, Fig. 6-5, and Fig. 6-6 was expressed as normal distribution curves in terms of percent change in parameter. This information was plotted directly as Fig. 6-7, Fig. 6-9, and Fig. 6-11. The material from these figures was replotted as Fig. 6-8, Fig. 6-10, and Fig. 6-12.

Fig. 6-13 through Fig. 6-16 represent the transistor characteristic curves in which $I_c$ is plotted as a function of $V_c$ for a constant $I_b$. Three runs are represented. Runs five and seven trace the growth of $I_{co}$ as radiation dose increases. This effect is shown by the characteristic upward fanning of the curves. In the case of these runs the oscillator was irradiated until failure. Run four is represented in Fig. 6-15 and Fig. 6-16. This circuit was not run until failure, but the fan effect was well developed when the circuit was removed from the gamma environment, Fig. 6-15.

The annealing effect is shown in Fig. 6-16. It may be seen that that family of curves follow an erratic path in their recovery. After 300 hours of annealing, the transistor appears to have returned to normal.

The radiation effects on the output frequency of a transistor R-C phase-shift oscillator were predicted by applying the results of radiation tests on individual components to the analysis of the linear model of the circuit presented in Chapter 4. For the experimental circuit shown in Fig. 3-1, mica capacitors and wire wound resistors were used for reasons summarized in Chapter 2. As predicted the capacitors and resistors did not change values under radiation levels that destroyed the effectiveness of the

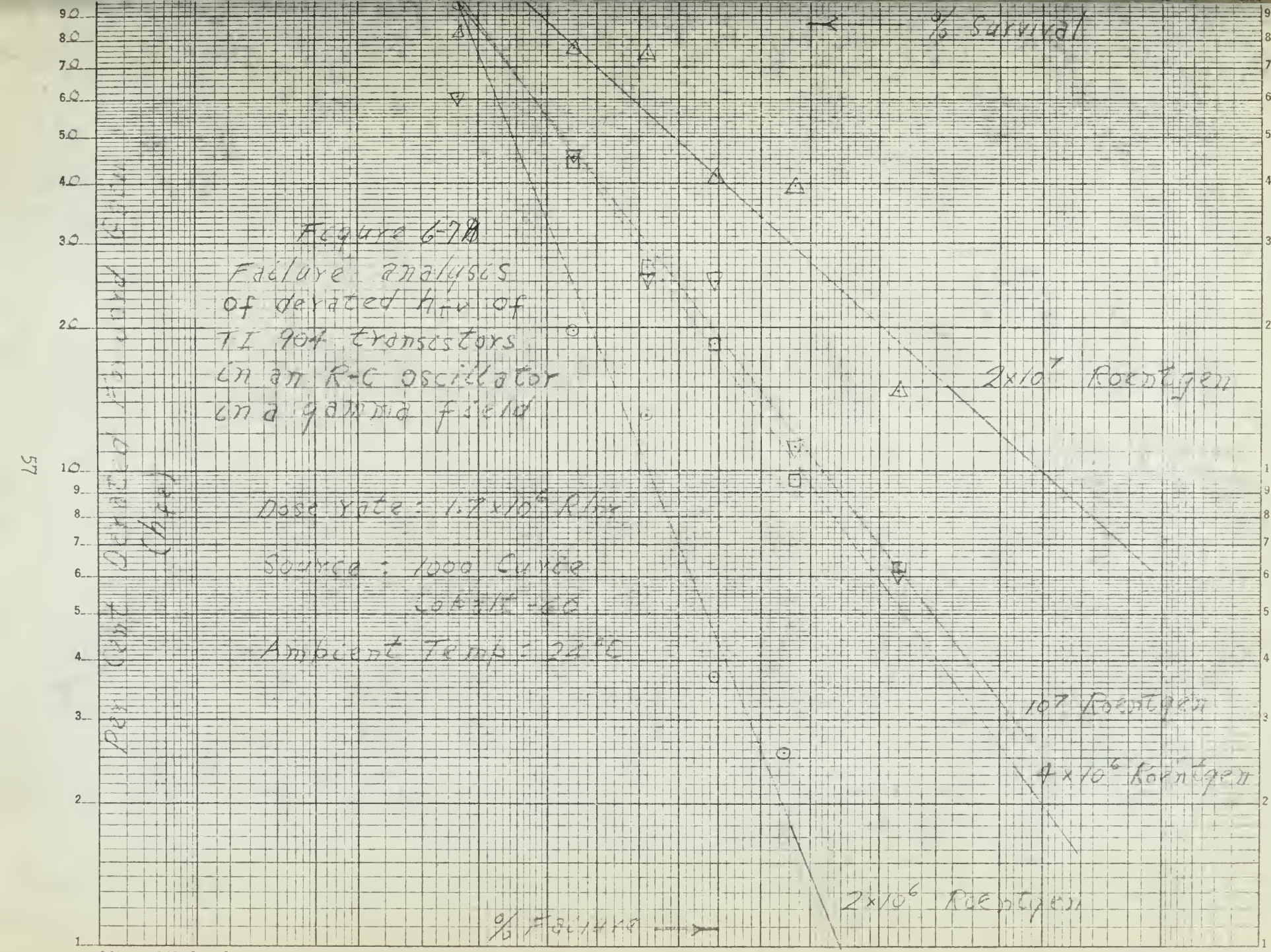


Figure 6-78
Failure analysis of derated h_FE of TI 904 transistors in an R-C oscillator and gamma field

Dose rate: 1.7×10⁶ R/hr
Source: 1000 Curie Co⁶⁰ TF-62
Ambient Temp: 22°C

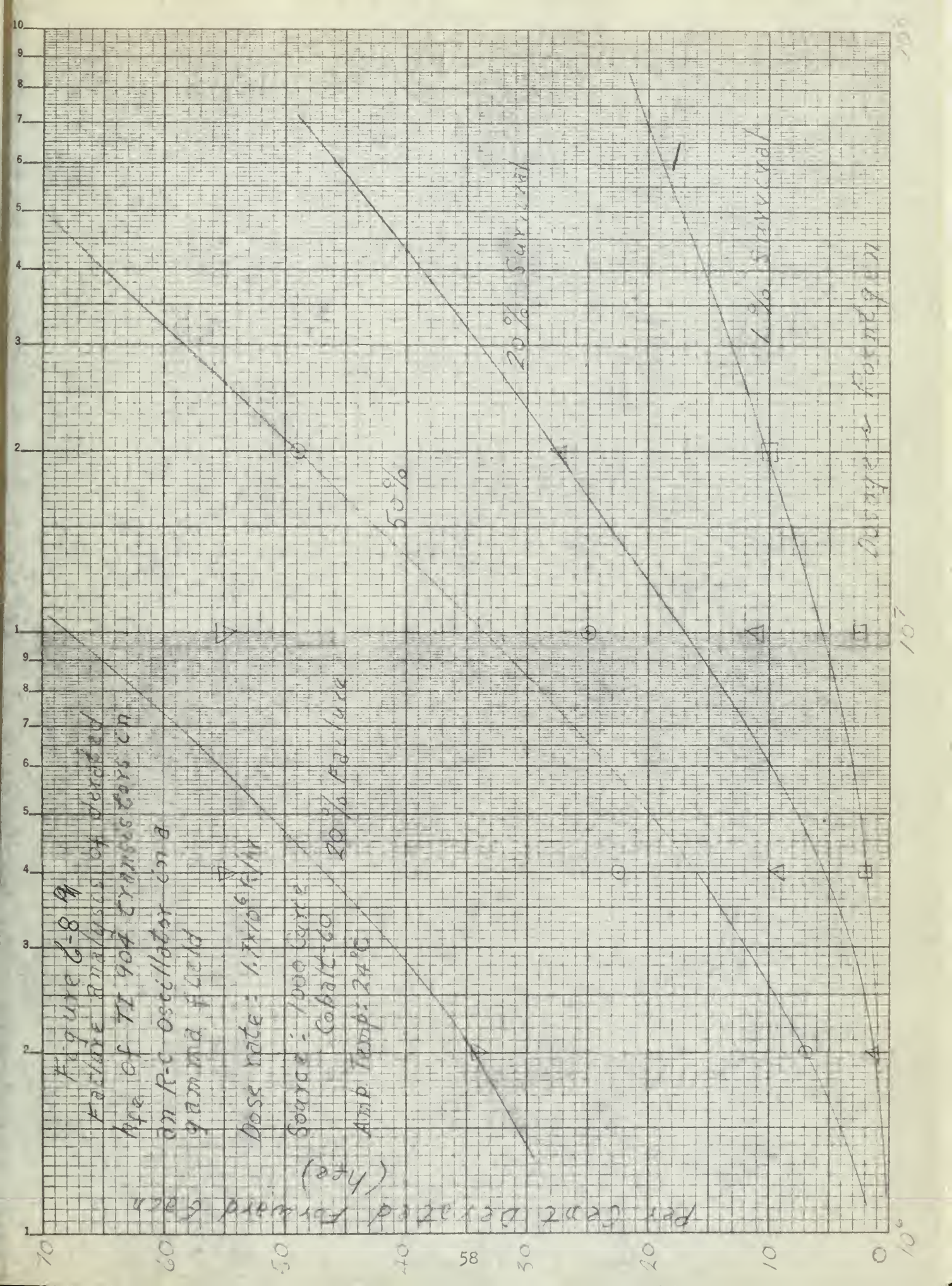
Figure 2-8 (a)
Dose rate of Tl 201 2 mm thick lead shielded source as a function of distance
Dose rate: 1.7 rad/hr
Source: 1 curie
20% radiation
Air temperature 22°C
(feet)
Percent Decrease Per Unit Distance
1
20%
50%
10
9
8
7
6
5
4
3
2
1
70
60
50
40
30
20
10
0
58

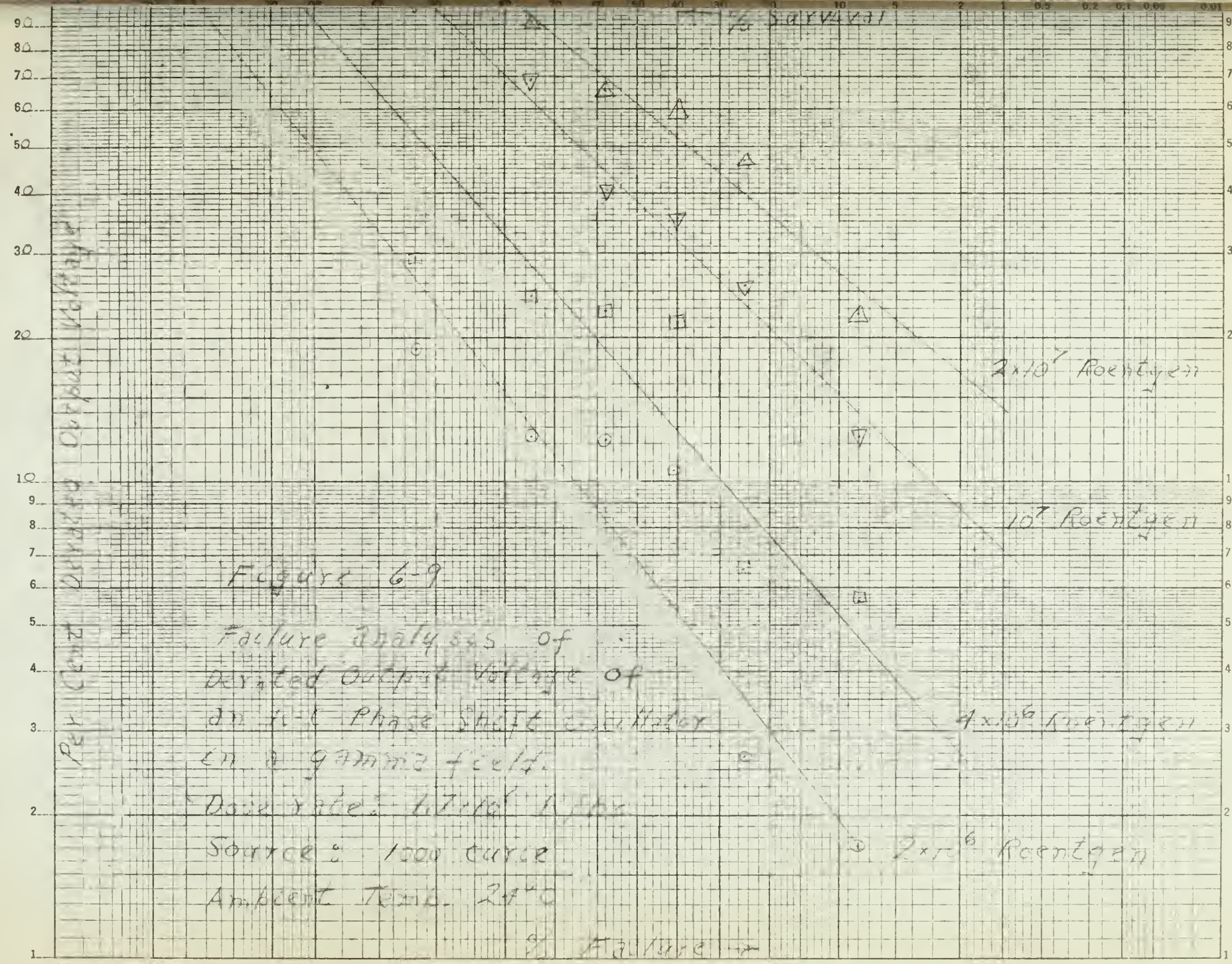


Figure 6-9

Failure analysis of derated output voltage of an A-C phase shift converter on a gamma field.

Dose rate: 4.1×10^5 r/hr

Source: 1000 curie

Ambient Temp: 24°C

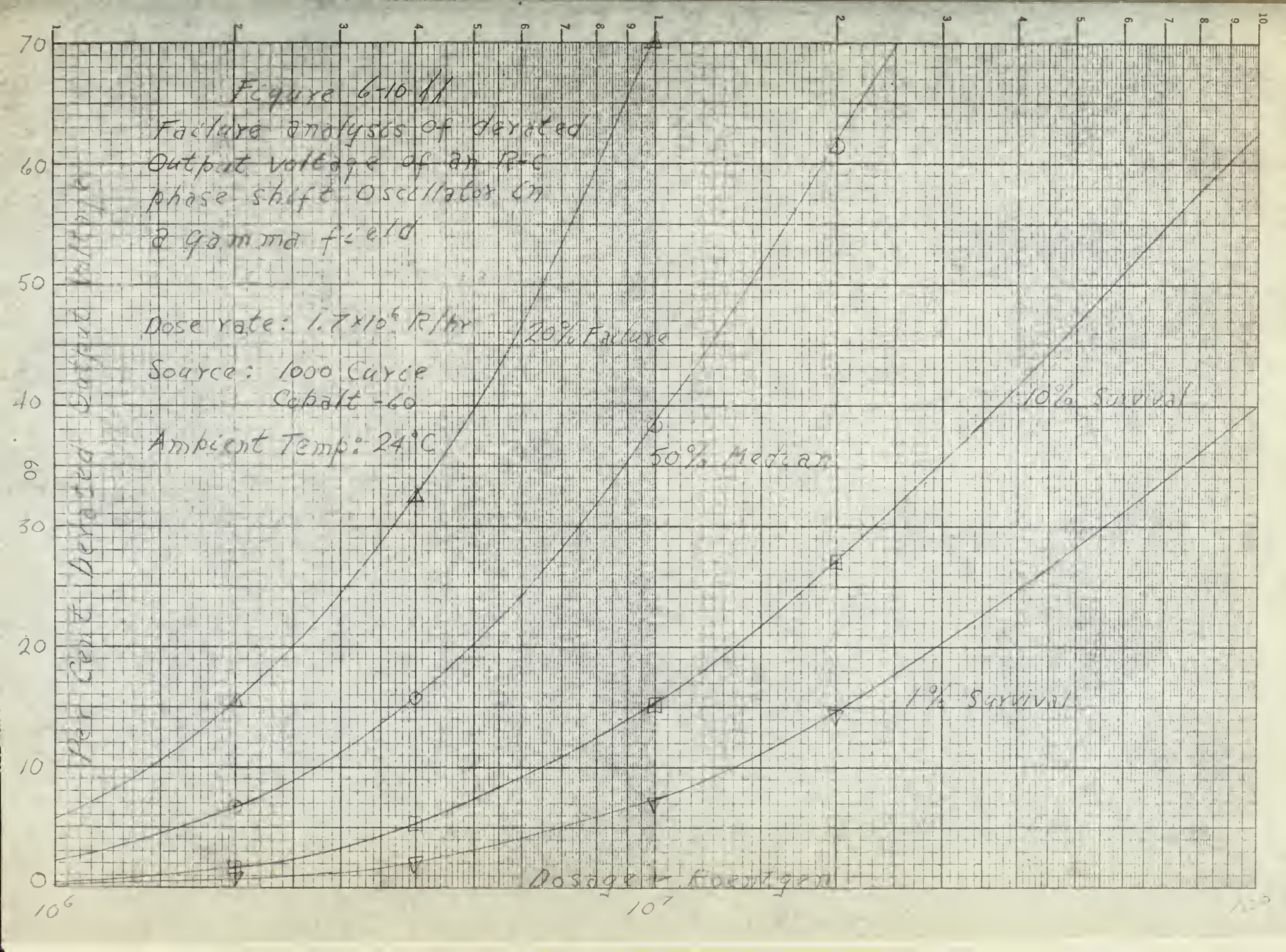
Figure 6-10 ff
Factors analysis of derated
Output voltage of an R-C
phase shift Oscillator in
a gamma field
Dose rate: 1.7×10⁶ R/hr
Source: 1000 Curie
Cobalt-60
Ambient Temp: 24°C
20% Failure
50% Median
10% Survival
1% Survival
Per Cent Derated Output Voltage
Dosage - Roentgen
70
60
50
40
30
20
10
0
10⁶
10⁷

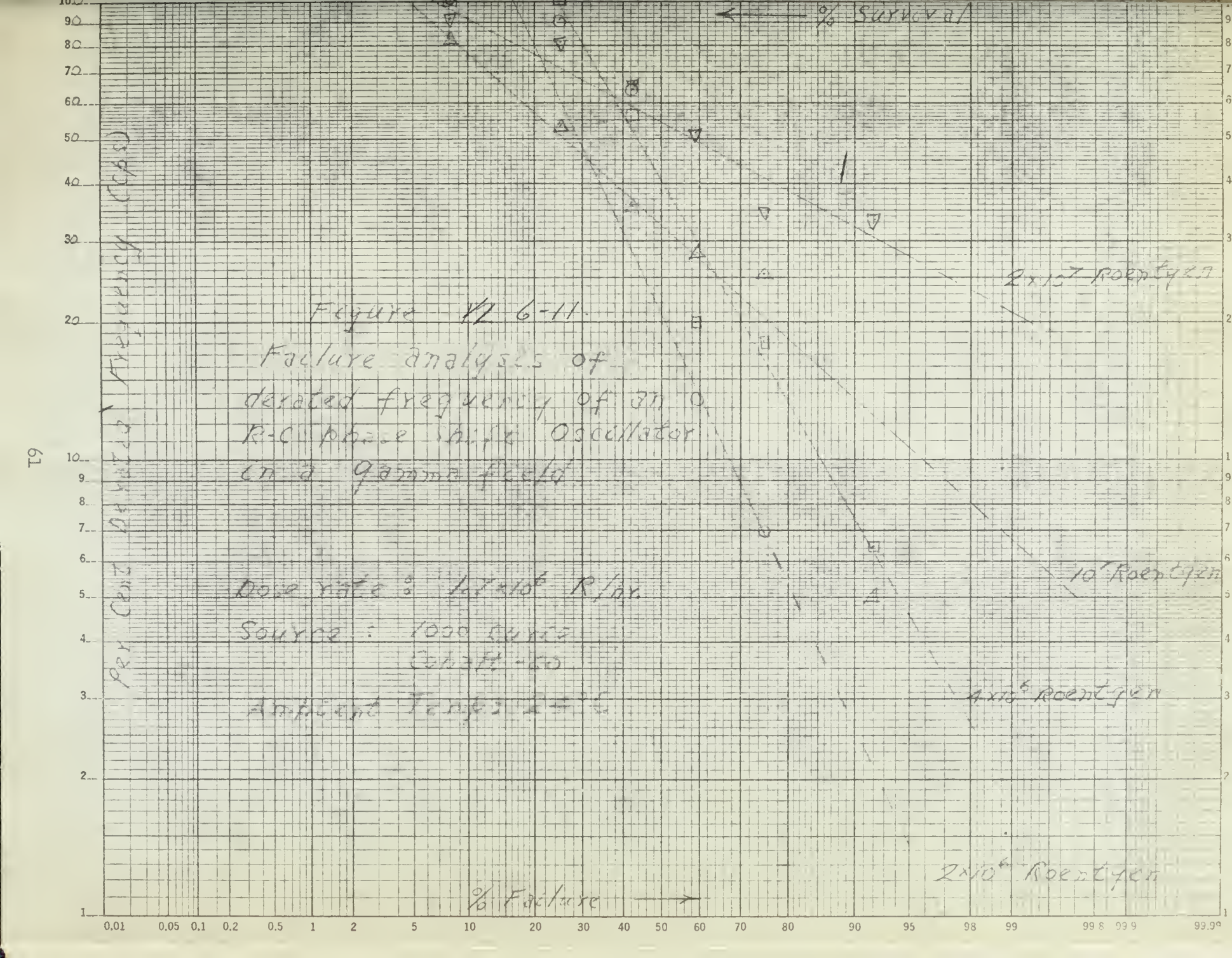


Figure # 6-11.

Failure analysis of detected frequency of an R-C phase shift Oscillator in a gamma field

Dose rate : $1.2 \times 10^6$ R/hr.

Source : 1000 curie Co$^{60}$

Ambient Temp : 25°C

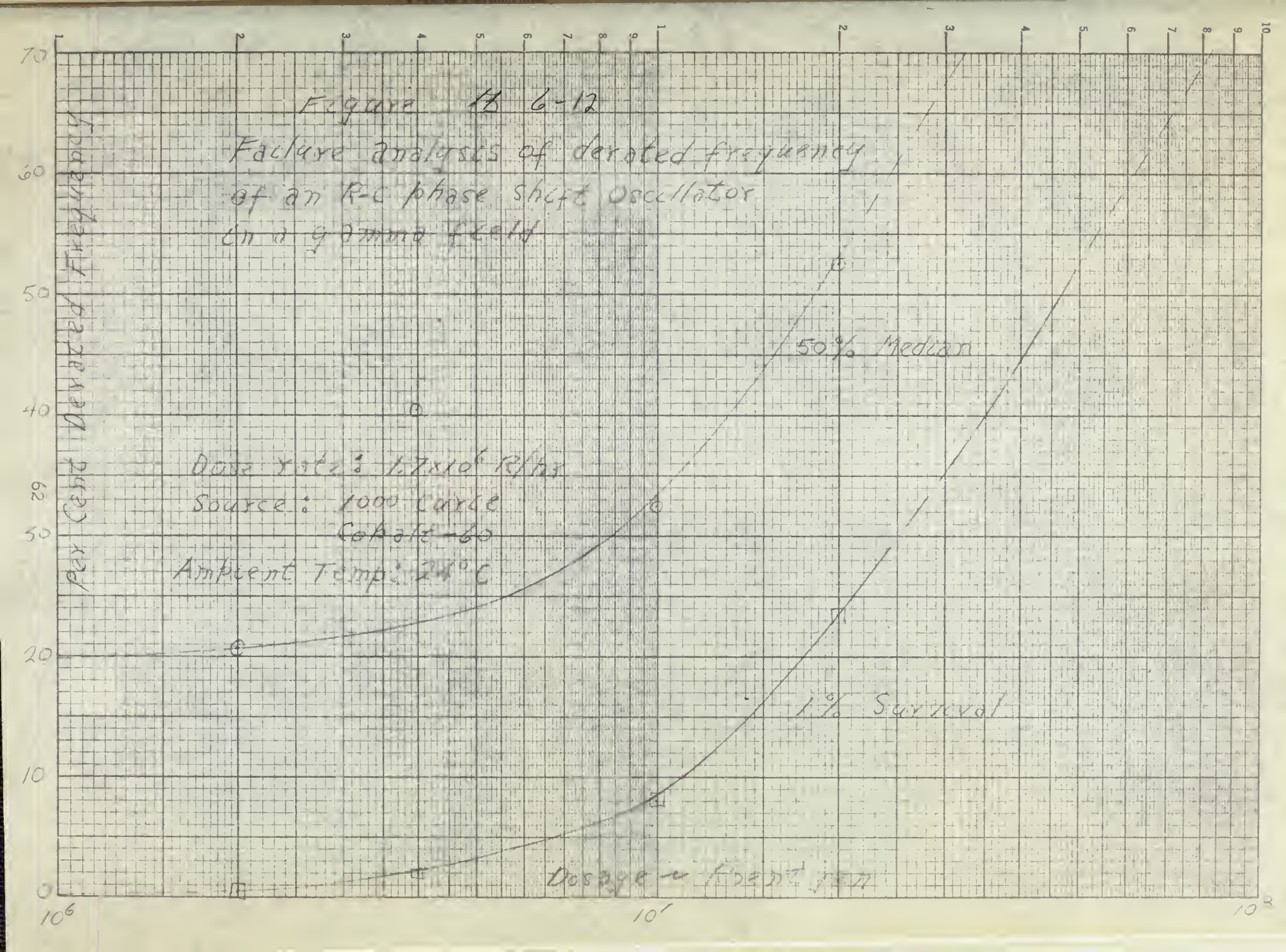
Figure 11 6-12
Failure analysis of derated frequency of an R-C phase shift oscillator in a gamma field
Dose rate: 1.7x10⁶ R/hr
Source: 1000 curie Cobalt-60
Ambient Temp: 24°C
50% Median
1% Survival
Dosage-Frequency
Percent Failure
Failure Frequency
10⁶
10⁷
10⁸

Figure 6-13

Transistor curve tracer photographs in which $I_c$ is plotted against $V_c$ for a constant $I_b$. These graphs are for run number 5 and display the transistor characteristics of the TI 904 as it is being irradiated in a gamma flux of approximately $1.7 \times 10^6$ R/hr at an ambient temperature of 21 degrees centigrade.

$I_c$ -- .5 ma/div

$V_c$ -- 2 volts/div

$I_b$ -- . [illegible] a/step

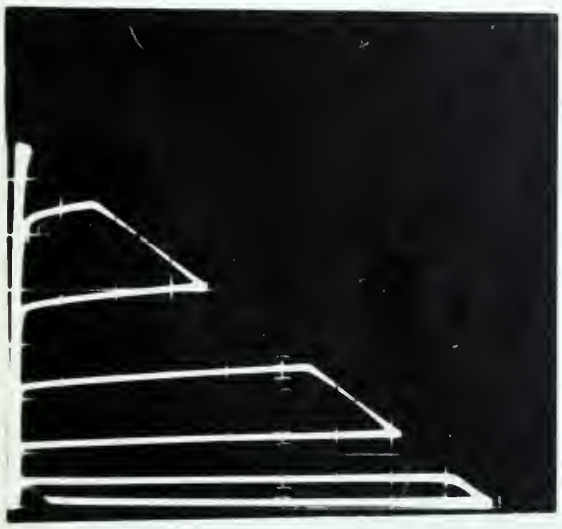

(a) Before irradiation

(b) After 30 minutes

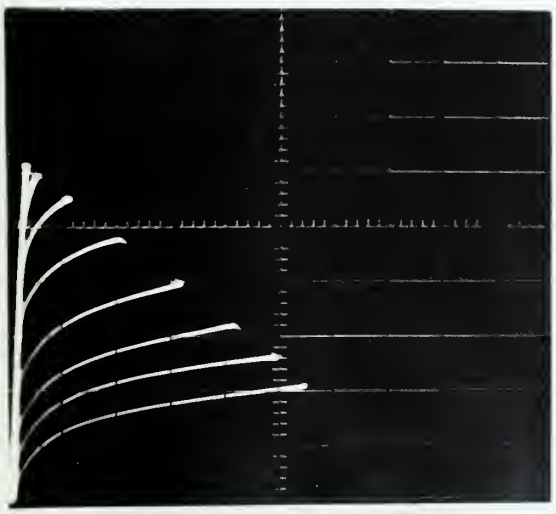

(c) After 5 hours

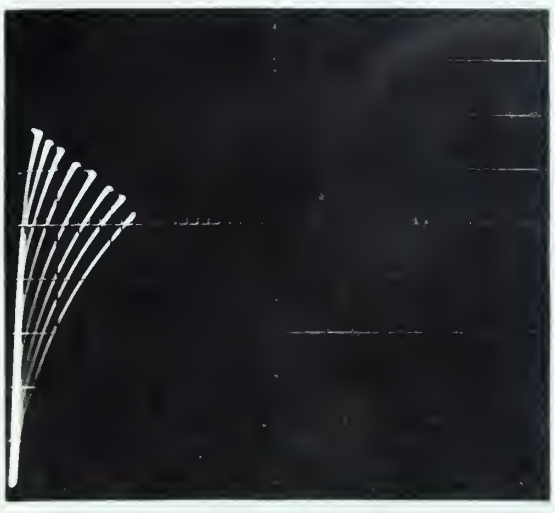

(d) After 16 hours

Figure 3-14

Transistor curve tracer photographs in which $I_c$ is plotted against $V_c$ for a constant $I_b$. These graphs are for run number 7 and display the transistor characteristics of the TI 904 as it is being irradiated in a gamma flux of approximately $1.7 \times 10^6$ R/hr for an ambient temperature of 24 degrees centigrade.

$I_c$ -- .5 ma/div

$V_c$ -- 2 volts/div

$I_b$ -- .02 ma/step

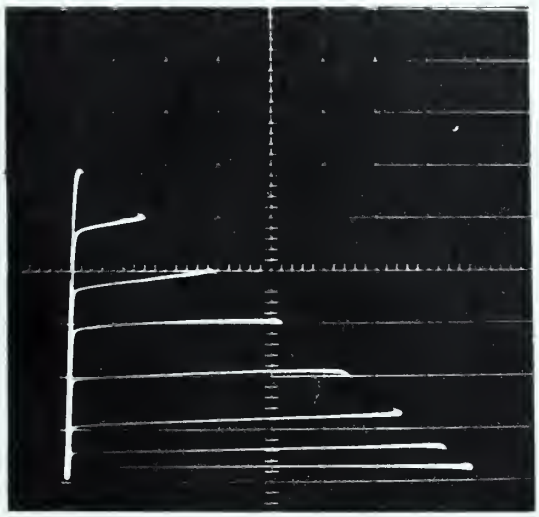

(a) Before Irradiation

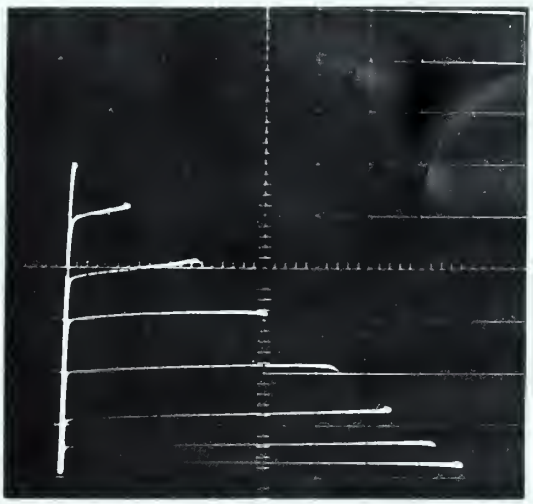

(b) After 5 minutes

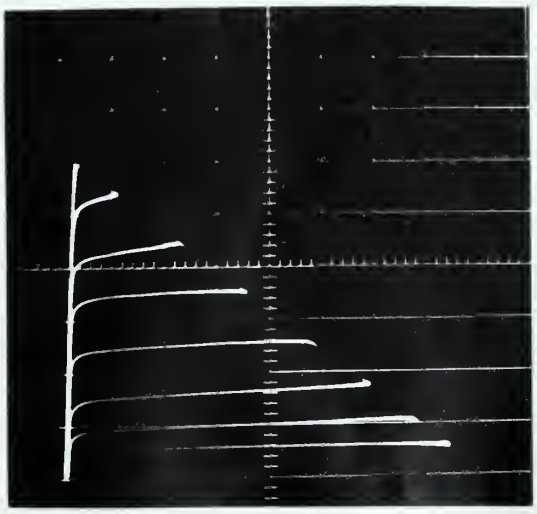

(c) After 1 hour

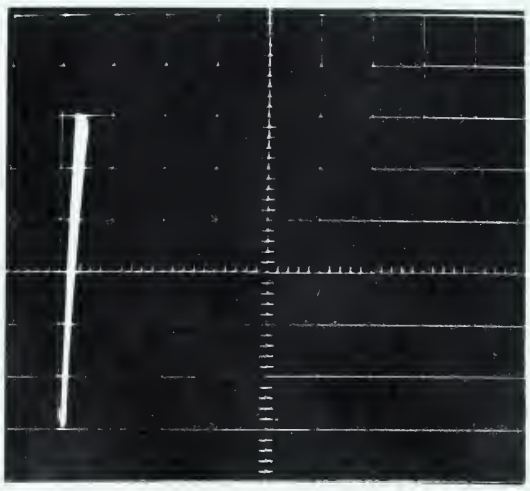

(d) After 12 hours

Figure 6-15

Transistor curve tracer photographs in which $I_c$ is plotted against $V_c$ for a constant $I_b$. These graphs are for run number 4 and display the transistor characteristics of the TI 904 just before and immediately after 23 hours of irradiation in a gamma flux of approximately $1.7 \times 10^6$ R/hr at an ambient temperature of 24 degrees centigrade.

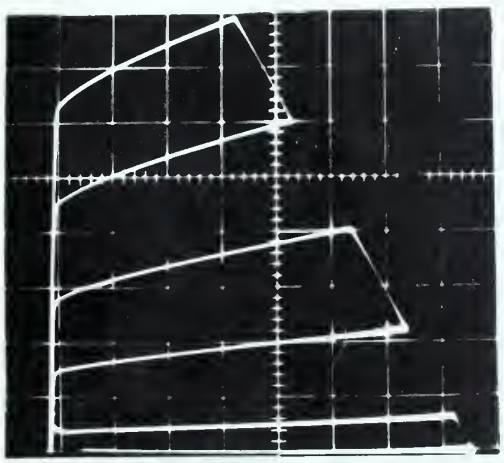

(a) Before irradiation

$I_c$ -- 2 ma/div

$V_c$ -- .2 volts/div

$I_b$ -- .01 ma/step

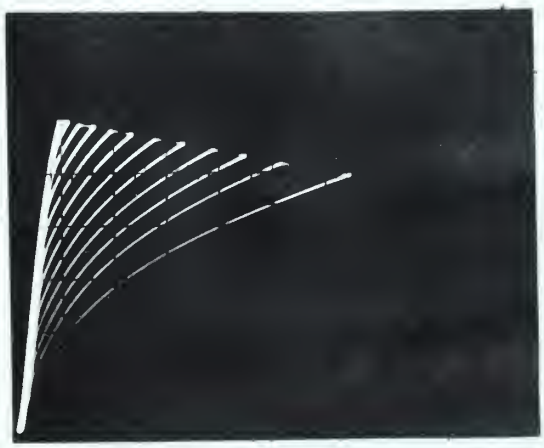

(b) After 23 hours

$I_c$ -- .5 ma/div

$V_c$ -- .2 volts/div

$I_b$ -- .01 ma/step

Figure 6-16

Transistor curve tracer photographs in which $I_c$ is plotted against $V_c$ for a constant $I_b$. These graphs are for run number 4 and display the transistor characteristics of the TI 904 as it undergoes annealing after removal from the gamma flux.

$I_c$ -- .5 ma/div

$V_c$ -- .5 volts/div

$I_b$ -- .01 ma/step

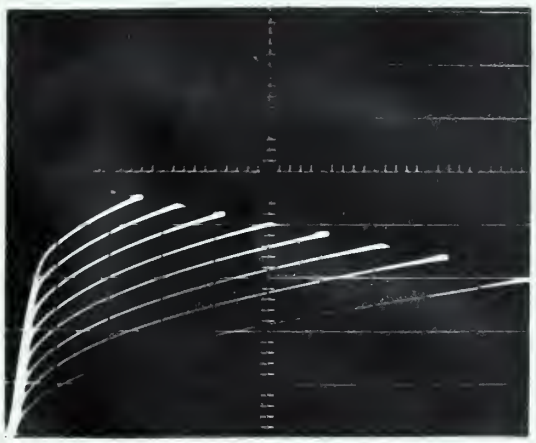

(a) 30 hours after removal

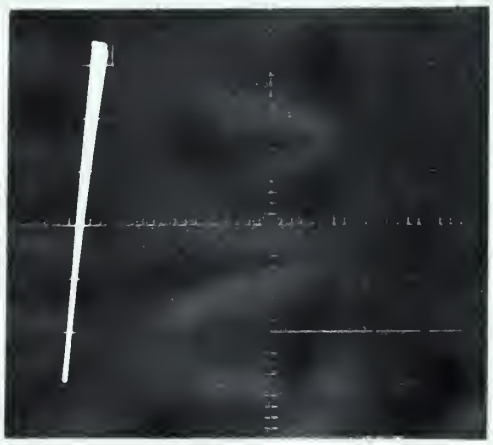

(b) 89 hours after removal

(c) 300 hours after removal

transistor. The transistor selected (T.I. 904) was known to be relatively sensitive to radiation. The transistor current gain degraded under radiation in a manner that in general was predicted by Keister and Stewart, Ref. 8. See Fig. 6-4. Using the results of the analysis, particularly Fig. 4-15, a plot of frequency against current gain, $h_{fe}$, was made as shown in Fig. 6-17. Adjustment was made to the original value of the capacitors because of the capacity of the test leads. The capacitors were no longer equal but ranged in values from 0.0080uf to 0.0085uf. For the prediction of frequency range all the capacitors were assumed equal at a value of 0.00825uf. For comparison, the experimental results of the first irradiated circuit is also plotted on Fig. 6-17. The variation of the experimental results from the theoretical prediction can be explained by one or all of the following reasons:

1. the capacitors were not equal;
2. the action of the transistor was non linear;
3. graphical approximations were made.

It is noted that the operation and frequency stability of the circuit can be increased by selecting a more radiation resistant transistor guided by criteria suggested in Chapter 2. It is also noted from Fig. 4-12 that the frequency stability of a transistor phase-shift oscillator will be increased by designing the circuit to use a high gain transistor.

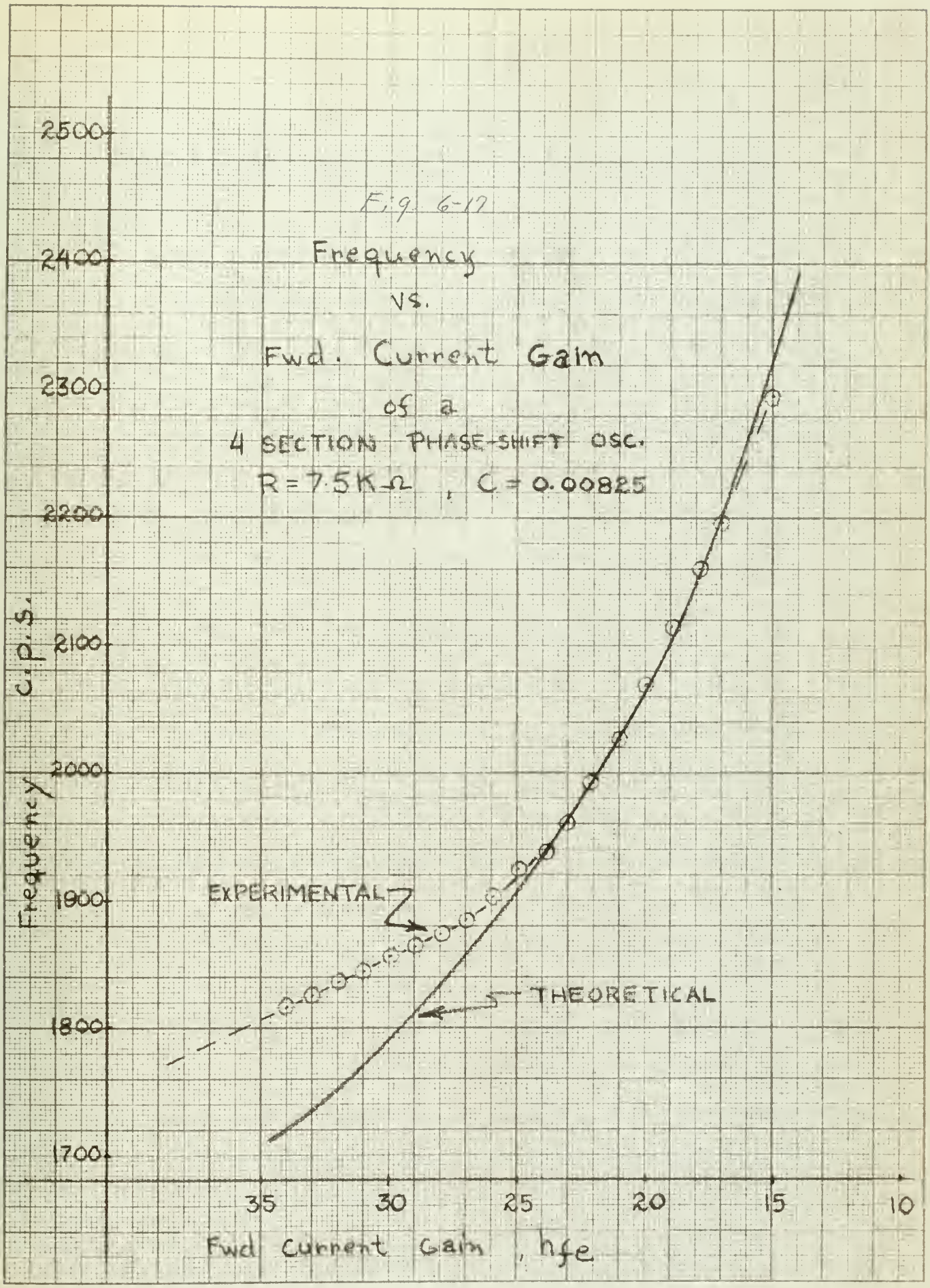
Fig. 6-17
Frequency
vs.
Fwd. Current Gain
of a
4 SECTION PHASE-SHIFT OSC.
R = 7.5K Ω , C = 0.00825
2500
2400
2300
2200
2100
2000
1900
1800
1700
C.P.S.
Frequency
EXPERIMENTAL
THEORETICAL
35
30
25
20
15
10
Fwd Current Gain , hfe

CHAPTER 7

## Conclusions

The following conclusions may be made from the results of the investigation.

1. The transistor was the most sensitive component.
2. No changes were observed in the resistors or capacitors.
3. The critical dosage where most parameters showed a break toward a more rapid change was $10^7$ roentgen.
4. The Texas Instrument 904 transistor exhibited the following characteristics under gamma radiation.
   a. $h_{ob}$ remained essentially constant at its initial value with a slight rise in value as the circuit failed.
   b. $h_{rb}$ exhibited the same tendencies as $h_{ob}$.
   c. $h_{ib}$ exhibited a constant rise during irradiation.
   d. $h_{fe}$ was essentially constant at its initial value until a dose of $3x10^6$ roentgens was obtained and then it exhibited a linear decrease.
5. The characteristics of the phase-shift oscillator varied under radiation in the following manner.
   a. Output voltage exhibited two general decay slopes with the break being at about $10^7$ roentgens.
   b. Frequency exhibited continual rise with marked peaking near the end followed by a sudden drop off.
6. The above results can be generally predicted by applying the results of radiation tests on individual components to circuit analysis.

# RECOMMENDATIONS

The frequency stability of the transistor RC phase-shift oscillator in a radiation environment can be improved in the following manner:

1. the use of radiation resistant components;
2. the use of a transistor with high current gain;
3. the design of a circuit such that it will operate effectively with high gain transistor.

BIBLIOGRAPHY


1941 E. L. Ginzton and L. M. Hollingsworth, "Phase-Shift Oscillators", Proc. I.R.E., 29, 43-49, February 1941.

1944 M. Artzt, "Frequency Modulation of Resistance-Capacitance Oscillators", Proc. I.R.E., 32, 409-414, July 1944

1949 W. C. Vaughn, "Phase-Shift Oscillators", Wireless Eng., 26, 391-399, December 1949.

1950 W. R. Hinton, "The Design of R.C. Oscillator Phase Shifting Networks", Electronic Eng., 22, 13-17, January 1950

1953 W. Edson, Vacuum Tube Oscillators , John Wiley, New York, 1953.

S. J. Mason, "Feedback Theory--Some Properties of Signal Flow Graphs", Proc. I.R.E., 41, 9, p. 1144, 1953.

1954 W. R. Evans, Control System Dynamics , McGraw-Hill Book Co. Inc., New York, 1954.

1955 J. G. Truxal, Automatic Feedback Control System Synthesis. McGraw-Hill, 1955.

1956 W. Hicks, "Transistor Phase-Shift Oscillator," Tele-Tech and Electronic Industries, July, pp 55-56, 1956.

G. L. Keister, H. V. Stewart, et al, "Preliminary Report of an Investigation of the Effects of Nuclear Radiation on Selected Transistors and Diodes," Boeing Airplane Co. Report D5-1183, dated 22 August, 1956.

S. J. Mason, "Feedback Theory--Further Properties of Signal Flow Graphs," Proc. I.R.E., 44, 7, p. 92c, 1956.

M. H. Nichols and L. L. Rauch, Radio Telemetry , 2nd Ed., John Wiley, New York, 1956.

J. C. Pigg and C. C. Robinson, "Radiation Effects in Semiconductor Devices," Preceedings of the Transistor Reliability Symposium, Sept. 17 & 18, 1956, New York University Press, New York, 1958.

H. L. Steele, Jr., "Effects of Gamma Radiation on Transistor Parameters," Proceedings of the Transistor Reliability Symposium, Sept. 17 & 18, 1956, New York University Press, New York, 1958.

R. P. Turner, "Transistorized Phase-Shift Oscillator", Radio and Television News, p. 108, April 1956.

O. Wing, "Ladder Network Analysis by Signal Flow Graphs", Trans. I.R.E. P.G.C.T., CT-3, p. 289, 1956.

1957 J. H. Crawford and J. W. Cleland, "Radiation Effects in Semiconductors," pp. 67-108, Progress in Semiconductors, Vol. 2, John Wiley, New York, 1957.

Decker, Solid State Physics, Prentice-Hall, New York, 1957.

C. T. Dienes and C. H. Vineyard, Radiation Effects in Solids, Interscience Publishers, New York, 1957.

Etherington, Nuclear Engineering Handbook, McGraw-Hill, New York, 1957.

J. F. Hansen, S. E. Harrison, and W. L. Hood, The Effect of Nuclear Radiation on Electronic Components and Systems, The Radiation Effects Information Center, Battelle Memorial Institute, Columbus 1, Ohio, 1957.

W. W. Happ, "Signal Flow Graphs," Proc. I.R.E., 45, 9, p. 1293, 1957.

D. Holliday, Introductory Nuclear Physics, 2nd Ed., John Wiley, New York, 1957.

B. Reich and G. E. Pavlik, "A Survey of the Nuclear Radiation Effects on Semiconductor Materials and Devices," A.G.E.T. News Bulletin, p. 8-17, Vol. 1 No. 3, July 1957.

R. F. Shea, et al, Transistor Circuit Engineering, John Wiley, New York, 1957.

M. A. Xavier, et al, "Research to Determine the Effects of Nuclear Radiation on Semiconductor Electronic Components," Report #2, 18 February, 1957; Report #3, 10 June, 1957, Inland Testing Labs Report. Division of Cook Electric Company, 1957.

1958 W. W. Happ, "A New Teaching Air: Flow Graphs," Lockheed Aircraft Corp., LMSD2416, Palo Alto, California, 1958.

W. W. Happ and S. R. Hawkins, "A Critical Survey of Radiation Damage to Circuits," A Report for Lockheed Aircraft Corp., LMSD5032, Palo Alto, California.

W. W. Happ and S. R. Hawkins, "Radiation Damage to Transistor Circuits," Interim Report, Lockheed Aircraft Corp., LMSD5032, Palo Alto, California.

J. B. Hoag, et al, Nuclear Reactor Experiments, D. Van Nostrand Co., Princeton, New Jersey, 1958.

Hurley, Junction Transistor Electronics, John Wiley, New York, 1958.

1958 V. M. Luibin, "Transistor RC-Oscillators with Phase Reversal," pp. 60-69, Radio Engineering, Vol. 13, #2, 1958, A Technical and Theoretical Journal of A.S. Popov Technical Society of Radio Engineering and Telecommunications, Translated by Forgonan Institute, New York.

T. R. Nisbet and W. W. Happ, "Flow-Graph Analysis--A Visual Form of Engineering Mathematics," Technical Report LMSD 48357, Lockheed Aircraft Corporation, Sunnyvale, California, 1958.

H. L. Steele, Jr., "Cobolt-60 Gamma Radiation Effects in Transistors," Report #D2-1201, Boeing Airplane Company, August 21, 1958.

E. Wolfendale, The Junction Transistor and its Applications, Heywood and Company LTD., London, 1958.

1959 T. R. Nisbet, "Effects of Radiation on Electronic Equipment," LMSD 48498, Lockheed Aircraft Corporation, March 18, 1959.

A. J. Heeger, T. R. Nisbet, W. W. Happ, "An Estimate of Transistor Life in Satellite Applications," Proc. I.R.E., Vol. 47, No. 5, May 1959.

Appendix I

Flow Graph Analysis

A. Definition

A flow graph is a graphical representation of a system of variables. Each variable is designated by a node. The rule relating two variables or nodes is called the transmittance. A transmittance is a directed line between two nodes with a value assigned which denotes the effect of the independent variable on the dependent one. An independent variable is represented by a departure node and a dependent variable corresponds to a target node.

B. Operations

1. By definition, there exists the following operations:

a. Multiplication.

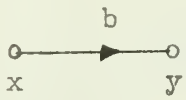


$y = bx$

note also the unit transmittance


$y = x$

b. Addition.

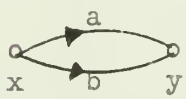


$y = (a + b)x$

or

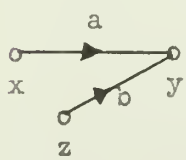


$y = ax + bz$

2. The following operations can be derived:

a. Division.

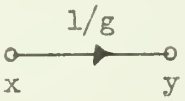


$y = x/g$

b. Subtraction

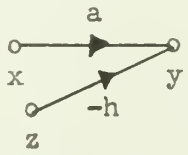


$y = ax - hz$

c. Feedback.

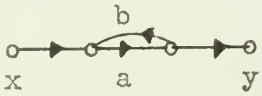


$$y = \frac{a}{1-ab}\, x$$

or

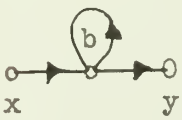


$$y = \frac{1}{1-b}\, x$$

note the <u>loop</u> formed by feedback.

C. <u>Further definitions</u>

1. Types of flow graphs.

a. An <u>open</u> flow graph has at least one departure node and one target node.

b. A <u>closed</u> flow graph is one in which the target node is also the departure node.

2. Loop.

a. A <u>loop</u> is a closed continuous sequence of transmittances in the same direction which touch each node only once.

b. The <u>value</u> of a loop is the product of the transmittances which form it.

3. Topology equation.

a. At any point in a closed flow graph, the flow leaving the point is always identical to the flow entering it. Therefore,

$$\sum_{n=0}^{\infty} (-1)^n L_n = 0$$

where $L_n$ = The value of each $n^{th}$ order loop present in a given system.

hence $L_0 = 1$

$L_1$ = The sum of the values of all simple loops.

$L_2$ = The sum of the values of all non-contiguous first order loops.

b. The topology equation provides the characteristic equation of closed flow graphs.

4. Non-Touching rule.

a. $$T = \sum_{j=0}^{\infty} \frac{P_j L_j}{L}$$

where $L_j = \sum_{n=0}^{\infty} (-1)^n [L_j]_n$, the value of all loops not touching $j^{th}$ path.

$L$ = Topology equation.

$P_j$ = $j^{th}$ path.

$n$ = order of the loops.

b. Useful in evaluating open flow graphs.

D. Procedure

1. Draw schematic diagram of the physical system.

2. Draw flow graph.

   a. Build from simple flow graphs that are derived from the simplest relationships of the variables.

   b. Check for compatibility.

      i. Does every variable and parameter appear with correct relationships?

      ii. Is each node in the flow graph defined?

3. Evaluate the transmittance of the system by using appropriate rules.